Modelling morphodynamic development in the presence of immobile sediment

Chavarrías, Víctor; Ottevanger, Willem; Sloff, C.J.; Mosselman, E.

DOI
10.1016/j.geomorph.2022.108290

Publication date
2022

Document Version
Final published version

Published in
Geomorphology

Citation (APA)
Chavarrías, V., Ottevanger, W., Sloff, C. J., & Mosselman, E. (2022). Modelling morphodynamic development in the presence of immobile sediment. *Geomorphology*, *410*, Article 108290. https://doi.org/10.1016/j.geomorph.2022.108290

Geomorphology 410 (2022) 108290

Contents lists available at ScienceDirect

Geomorphology

journal homepage: www.journals.elsevier.com/geomorphology

Modelling morphodynamic development in the presence of immobile sediment

Víctor Chavarrías [a,*], Willem Ottevanger [a], Kees Sloff [a,b], Erik Mosselman [a,b]

[a] Deltares, Boussinesqweg 1 2629 HV Delft, the Netherlands
[b] Faculty of Civil Engineering and Geosciences, Delft University of Technology, Stevinweg 1 2628 CN Delft, the Netherlands

ARTICLE INFO

Keywords:
Mixed-size sediment
Immobile sediment
Fixed layers
Coarse layer
Active-layer model

ABSTRACT

Predicting the formation and break-up of immobile layers is of crucial importance for river management, as these processes greatly affect the morphodynamic evolution of the river bed. Two models are currently available for studying these processes: Struiksma's and Hirano's model. In this paper, we show that both models present limitations. This is done by numerical modelling of a laboratory experiment and two thought experiments. Struiksma's model does not predict break-up and Hirano's model yields unrealistic results when part of the sediment is immobile. We propose two alternatives that overcome these limitations: the ILSE and HANNEKE models. They differ in the interpretation of the top part of the bed interacting with the flow. Moreover, only the HANNEKE model explicitly predicts the formation of coarse layers, at the expenses of a more limited application range.

1. Introduction

Alluvial rivers respond to environmental changes and human interventions by changing their geometry or their bed sediment composition, or both. Numerical models to simulate these processes are well established. They commonly compute the changes in bed sediment composition through Hirano's, 1971 approach by which non-cohesive mixtures of grain sizes are divided into distinct size fractions. Mass conservation and transport of sediment are computed for an active top layer of the riverbed, accounting for the interactions between grains of different sizes through hiding and exposure. Complications arise when part of the sediment becomes immobile as shear stresses exerted on larger grains fall below the corresponding threshold of motion. For instance, the accumulation of coarser sediment in the troughs of underwater dunes by winnowing (Carling et al., 2000a, 2000b) may develop into an immobile layer, partly covered by dunes of mobile finer sediment that travel over this layer. The formation and break-up (Klaassen et al., 1986; Klaassen, 1987) of immobile layers varies in time and space and thus greatly affects the morphodynamic evolution of the river bed. This is important for river management, as illustrated by several examples from the river Rhine. First, the development of the major Rhine bifurcation at Pannerden depends sensitively on the sediment transport and composition patterns in the bifurcation area (Sloff and Mosselman, 2012). This development governs the water supply, the navigability and the flooding risk along different branches of the Rhine delta. Second, fixed riprap layers have been implemented to improve the navigability of Rhine bends at Nijmegen and Sint-Andries (Sloff et al., 2006; Havinga, 2020). Mobile sediment transported over these fixed layers poses similar problems to modelling as mobile sediment transported over naturally formed immobile layers. Third, sediment augmentation to arrest bed degradation (Bravard et al., 1999; Visser, 2000; Siele et al., 2019; Becker, 2017; De Jong and Ottevanger, 2020) might be more effective if the added sediment would be coarser than the material of the bed, because it would result in a steeper longitudinal equilibrium profile, incising less deep, as well as a flatter transverse bed profile, increasing the width for navigation (Mosselman et al., 2004). However, the coarser sediment might develop into immobile layers with undesired effects. Finally, interactions between mobile sediment and an immobile armour layer caused concerns in the Old Rhine (Rest-Rhein, Vieux Rhin) at the border between France and Germany. Nourishment of sediment for ecological reasons (Die Moran et al., 2013; Arnaud et al., 2015, 2017; Staentzel et al., 2018) was feared to trigger further river incision by breaking up the armour layer (Figs. 1 and 2), rendering flood retention polders along the river (e.g. Peters et al., 2001) ineffective.

Hirano's, 1971 model is appropriate for conditions when all size fractions of the sediment mixture are mobile. Struiksma (1999)

* Corresponding author.
E-mail address: victor.chavarras@deltares.nl (V. Chavarrías).

https://doi.org/10.1016/j.geomorph.2022.108290
Received 30 March 2021; Received in revised form 20 February 2022; Accepted 6 April 2022
Available online 4 May 2022

developed a model for sediment transport over fixed layers that are never mobile. None of the two models can reproduce the formation of a coarse immobile layer explicitly. Tuijnder and Ribberink (2010b) developed a model for supply-limited sediment transport over immobile layers using results from their laboratory experiments, but the validity of this model was found to be limited to the conditions of the experiments (Chavarrías et al., 2020). Our objective is therefore to develop a more generally valid model for sediment transport and morphodynamic development in the presence of immobile sediment. We present two models for this: a simple modification of the Hirano model (ILSE) and a more complex modification (HANNEKE).

The paper is organized as follows. In Section 2, the Struiksma and Hirano models are explained. Section 3 is devoted to the two proposed models (i.e., ILSE and HANNEKE). In Section 4, the four models are compared and tested by reproducing a laboratory experiment. Two thought experiments inspired in the laboratory data set are also modelled. The modelling exercise highlights the capacity of the proposed models of capturing physical processes neglected by the existing models. Results are discussed in Section 5.

2. Existing mathematical models

2.1. Struiksma's model

Morphodynamic modelling is usually achieved by coupling the shallow water equations (e.g. Vreugdenhil, 1994) modelling flow with the mass balance equation for sediment:

$$\frac{\partial z_b}{\partial t} + \frac{\partial q_b}{\partial x} = 0 \tag{1}$$

in which t [s] is time, x [m] is the streamwise coordinate, z_b [m] is the bed elevation above a fixed datum z_0 [m], and q_b [m^2/s] is the total bed load transport per unit width expressed as sediment volume including pores (Fig. 3). For the sake of simplicity, we show the one-dimensional version of the system of equations. Implicit in using this equation is that compaction and dilation are irrelevant as well as uplift or subsidence (Paola and Voller, 2005).

The sediment transport rate is modelled by means of a closure relation as a function of the flow velocity, friction, and other bed properties (e.g. Meyer-Peter and Müller, 1948; Engelund and Hansen, 1967; Ashida and Michiue, 1971; Wilcock and Crowe, 2003). Hence, the sediment transport rate is assumed at capacity, neglecting retarded adaptation to capacity conditions due to sediment inertia (Bell and Sutherland, 1983; Jain, 1992). This assumption is valid for small concentrations of moving particles and when the adaptation timescale to changing flow conditions is fast with respect to changes in bed elevation (e.g. Armanini and Di Silvio, 1988; Garegnani et al., 2011, 2013). With the latter assumption, Eq. (1) yields the Exner (1920) equation:

$$\frac{\partial z_b}{\partial t} + \frac{dq_b}{du}\frac{\partial u}{\partial x} = 0 \tag{2}$$

where u [m/s] is the mean depth-averaged flow velocity. Eq. (2) implies also that the friction coefficient is independent of the flow depth. Otherwise, the sediment transport rate would depend on both the flow velocity and the flow depth, which would lead to an additional term.

Given that flow is modelled with the shallow-water equations (Barré de Saint-Venant (1871) in one dimension), the flow depth and flow velocity represent quantities averaged over length scales on the order of several times the flow depth. Hence, individual bedforms such as dunes, which scale with the flow depth, are not resolved. When using Eq. (2) in combination with a shallow-water model, the bed level must be interpreted as a mean averaged over the passage of several bedforms. The same interpretation holds for the sediment transport rate and all other variables.

Struiksma (1999) realized that Eq. (1) is not suitable for modelling conditions in which a non-erodible or fixed layer is exposed at the bed surface. Under these conditions, the sediment transport rate is smaller than according to relations derived for alluvial conditions. Struiksma (1999) proposed to consider a minimum sediment thickness above the fixed layer for which the conditions can be assumed alluvial (Fig. 4). When the sediment thickness is below this threshold, the sediment transport rate is reduced by a factor $\Psi \in [0,1]$ [−]. The reduction depends on the exposure of the fixed layer, which is modelled by the ratio between the actual sediment thickness δ [m] and the alluvial threshold thickness δ_a [m] (i.e., $\Psi = f(\delta/\delta_a)$).

Struiksma (1999) proposed a linear relation for Ψ such that:

$$\Psi = \begin{cases} \dfrac{\delta}{\delta_a} & \text{for} \quad \delta < \delta_a \\ 1 & \text{for} \quad \delta \geq \delta_a \end{cases} \tag{3}$$

Fig. 1. View of the Old Rhine (Rest-Rhein, Vieux Rhin).

In this case, the modified Exner (1920) equation is:

$$\frac{\partial z_b}{\partial t} + \frac{\partial \Psi q_b}{\partial x} = 0 \tag{4}$$

In the presence of dunes, the fixed layer will be exposed in the troughs. As the bed level is an average over several dunes, Ψ can be interpreted as the average fraction of the surface area in which the fixed layer is exposed. In this case, the alluvial threshold thickness is related to dune dimensions under alluvial conditions (i.e., unaffected by the presence of a fixed layer).

Two main limitations arise when using the model by Struiksma (1999). The first one is that the fixed layer can never be eroded regardless of the flow conditions. This is realistic when the fixed layer represents engineered riprap (e.g., the fixed layers at Sint Andries and Nijmegen in the Waal River in the Netherlands, Section 1). However, the application in Section 4 will show that the model is unsuitable for predicting morphodynamic development under conditions in which the layer of coarse sediment is only immobile under certain flow conditions.

The second limitation is that the properties of the fixed layer (i.e., the grain size) affect neither the sediment transport rate nor friction. In reality, the sediment transport rate over a fixed layer is hindered by the fact that grains are less exposed to the flow as they "hide" behind the larger grains of the fixed layer. This is part of the hiding-and-exposure effect known for mixed-size sediment (Einstein, 1950). Similarly, the friction experienced by the flow depends on the size of the sediment at the bed surface, which depends on the exposure of the fixed layer.

2.2. Hirano's model

Both the Exner (1920) and Struiksma (1999) models were devised for sediment with uniform grain sizes (uni-size sediment). Using these models, one cannot predict changes in bed surface composition (i.e., fining or coarsening of the bed surface in space and time). For modelling mixed-size sediment morphodynamic changes, Hirano (1971) developed the active-layer model. This can be interpreted as an extension of the Exner (1920) model. Sediment is represented by a discrete number N [−] of size fractions with characteristic grain sizes d_k [m], where increasing index values $k = 1, \cdots, N$ indicate increasing size. The total sediment transport is the sum of the transport of each size fraction q_{bk} [m^2/s]:

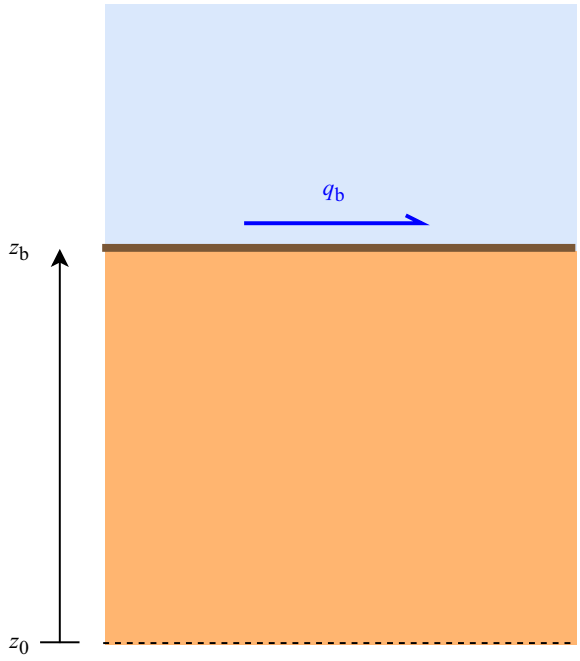

Fig. 3. Sketch of variables in model by Exner (1920).

$$q_b = \sum_{k=1}^{N} q_{bk} \tag{5}$$

The sediment transport per size fraction depends on the volume fraction content of size fraction k at the bed surface $F_{ak} \in [0,1]$ [−]:

$$q_{bk} = F_{ak} Q_{bk} \tag{6}$$

where Q_{bk} [m^2/s] is the sediment transport capacity. This is the sediment transport as if the bed surface would be composed of only size fraction k, yet accounting for the hiding-and-exposure effect (Deigaard and Fredsøe, 1978; Ribberink, 1987; Armanini, 1995).

Changes in bed elevation are modelled using Eq. (1). Modelling changes in bed surface composition (i.e., in F_{ak}) requires a mass balance

Fig. 2. Armoured bed of the Old Rhine (Rest-Rhein, Vieux Rhin).

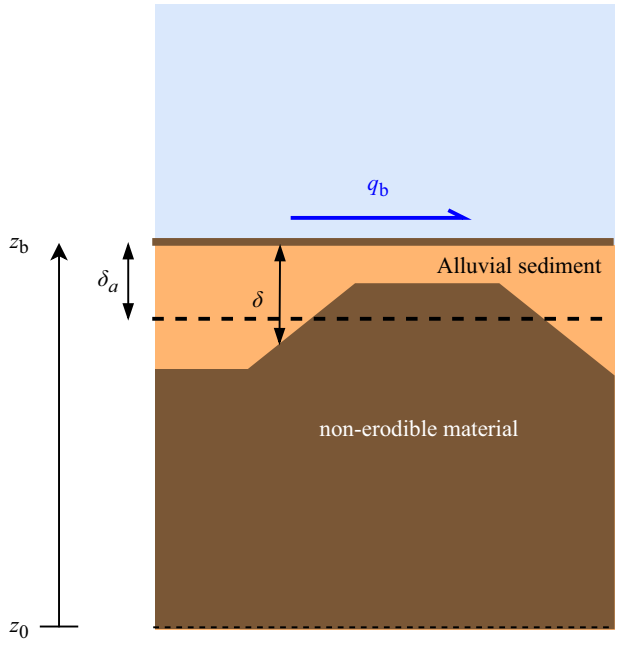

Fig. 4. Sketch of variables in model by Struiksma (1999).

equation for each sediment fraction at the bed surface. The vertical extent of the bed surface is assumed to have a thickness L_a [m] (i.e., the active-layer thickness) such that mass conservation of the active layer leads to equation:

$$\frac{\partial M_{ak}}{\partial t}+\frac{\partial q_{bk}}{\partial x}+\Phi_{sk}=0 \tag{7}$$

where $M_{ak}=F_{ak}L_a$ [m] is the volume of sediment in the active layer per unit of bed surface and Φ_{sk} [m/s] is the flux of sediment (including pores) between the active layer and the substrate sediment below (Fig. 5).

The mass balance of the substrate sediment between a fixed datum z_0 [m] and the interface between the active layer and the substrate at $z_s = z_b - L_a$ [m] yields:

$$\frac{\partial M_{sk}}{\partial t}-\Phi_{sk}=0 \tag{8}$$

where $M_{sk}=F_{sk}L_s$ [m] is the volume of sediment per unit of bed area in the substrate. $F_{sk}\in[0,1]$ [−] is the volume fraction content of size fraction k in the substrate and $L_s = z_b - L_a - z_0$ [m] is the substrate thickness.

For bookkeeping of stratigraphy, the substrate is numerically discretized into N_s layers of thickness l_{sl} [m], where $l=1,\cdots,N_s$ [−] is an index denoting substrate layer from top to bottom such that $L_s=\sum_{l=1}^{N_s} l_{sl}$. The volume fraction content of size fraction k in each bookkeeping layer is $f_{skl}\in[0,1]$ [−] and the volume of sediment per unit area is $m_s=f_{skl}l_{sl}$ [m].

The volume fraction contents add up to 1:

$$\sum_{k=1}^{N}F_{ak}=1,\sum_{k=1}^{N}F_{sk}=1,\sum_{k=1}^{N}f_{skl}=1\forall l \tag{9}$$

Under degradational conditions, sediment from the top of the substrate is transferred to the active layer. Under aggradational conditions, sediment in the active layer is transferred to the substrate:

$$\Phi_{sk}=\frac{\partial z_s}{\partial t}\begin{cases} f_{sk1} & \text{for} \quad \frac{\partial z_s}{\partial t}<0 \\ F_{ak} & \text{for} \quad \frac{\partial z_s}{\partial t}\geq 0 \end{cases} \tag{10}$$

Parker (1991) considers that the bed load composition affects the composition of the flux under aggradational conditions. This idea is encompassed by the flux described by Hoey and Ferguson (1994) in which a parameter $\alpha_s\in[0,1]$ weights the contribution of F_{ak} and the fraction of sediment in transport $F_{bk}=q_{bk}/q_b\in[0,1]$ [−] to the flux:

$$\Phi_{sk}=\frac{\partial z_s}{\partial t}\begin{cases} f_{sk1} & \text{for} \quad \frac{\partial z_s}{\partial t}<0 \\ \alpha_s F_{ak}+(1-\alpha_s)F_{bk} & \text{for} \quad \frac{\partial z_s}{\partial t}\geq 0 \end{cases} \tag{11}$$

The Hirano model crucially depends on the thickness of the control volume (i.e., the active-layer thickness). For a given sediment transport gradient, a thicker active layer will lead to smaller changes in bed

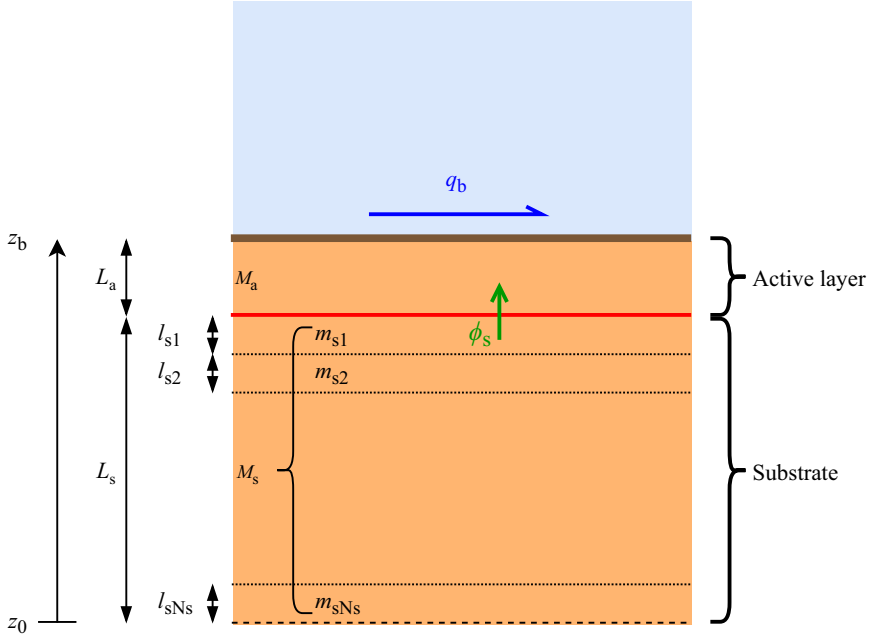

Fig. 5. Sketch of variables in the active-layer model by Hirano (1971).

surface composition, as the gradient becomes smaller relatively to the volume in the active layer.

As with all other model variables, the volume fraction content of sediment in the active layer is also an average over several bedforms not resolved by the flow. This means that mixing due to unresolved bedforms is not explicitly reproduced by the model. For this reason, the active-layer thickness is proportional to the part of the bed reworked in the time in which several unresolved bedforms pass. Under plane-bed conditions, the dominant unresolved bedforms causing mixing scale with the coarsest fractions in the bed. The active-layer thickness can then be taken proportional to D_{84} or D_{90} of the sediment mixture (e.g., Petts et al., 1989; Rahuel et al., 1989; Parker and Sutherland, 1990). Under dune-dominated conditions, dunes are the largest unresolved bedforms and the active-layer thickness can be taken proportional to the dune height (e.g., Deigaard and Fredsøe, 1978; Lee and Odgaard, 1986; Armanini and Di Silvio, 1988).

A general view of the active-layer thickness is achieved by considering a continuous measurement of the bed elevation. A mean bed elevation is obtained from the continuous measurement by averaging over several unresolved bedforms. The difference between the continuous measurement and the mean indicates the thickness of the bed reworked by bedforms. The active-layer thickness is usually set to 90–95% of the probability distribution of bed elevations fluctuations around the mean (Ribberink, 1987; Blom et al., 2003).

The active-layer thickness is often assumed to be constant (e.g. Bennett and Nordin, 1977; Ribberink, 1987; Papanicolaou et al., 2004; Cui, 2007; Hu et al., 2014). This is reasonable when considering that the vertical extent reworked by bedforms at the timescale and length scale under consideration is constant in both space and time. In general, dune properties or the characteristic grain size of the bed surface changes in both space and time. Hence, if these changes are relevant, the active-layer thickness is a function rather than a constant (e.g. Rahuel et al., 1989; Karim and Holly, 1986; Holly and Rahuel, 1990; Van Niekerk et al., 1992; Hoey and Ferguson, 1994; Wu, 2004).

The active-layer thickness does not refer to a layer that can be observed or measured in the field, but to the depth below the riverbed surface over which sediment is actively mixed. This depth of active mixing depends on the bedforms present and on the time scale considered. The active-layer thickness controls the celerity at which changes in grain-size distribution propagate through the domain (a thin active layer causes changes to propagate fast and vice versa). Hence, the active-layer thickness must be related to the dominant physical process responsible for the celerity of changes in grain-size distribution. The dominant physical process responsible for changes in grain-size distribution depends of the problem under consideration and the timescale of interest.

Suppose a case in which slightly finer sediment than the parent material is fed into a dune-dominated river. A fining wave will propagate in downstream direction. The celerity of the fining wave is better captured when scaling the active-layer thickness to dune height rather than grain size because in reality the fed sediment will vertically mix at the scale of the dune height and will not be restricted to the top $2D_{90}$ of the bed.

The active-layer thickness sets the part of the bed that interacts with the flow. This is essentially different from the bed load layer thickness (e.g. Van Rijn, 1984a; Luu et al., 2004; Wu and Yang, 2004; Colombini, 2004; Colombini and Stocchino, 2005) which represents the part of the bed that is moving. The sediment in the active layer is available for transport and sediment in transport deposits in the active layer. For this reason, the thickness of the bed load layer in a fully immobile bed is equal to zero, but the active-layer thickness is not zero.

Several other definitions of the active-layer thickness exist. For instance, Armanini and Di Silvio (1988) explain that sediment in the active layer is defined as the sediment that can be lifted (i.e., moved vertically) by the flow, contrary to the bedload layer where motion is primarily in the streamwise direction. The implications of the definition by Armanini and Di Silvio (1988) are the same as the ones previously introduced. In essence, the active-layer thickness depends on the predominant mixing process. Quoting Armanini and Di Silvio (1988):

> At the time- and space-scales relevant to the process, the continuous exchange of particles leaving and reaching the bottom involves not only the material presently subject to the water flow, but also the material bound to be exposed owing to the propagation of bedforms.

What we define as "sediment that interacts with the flow" is what they define as "sediment bound to be exposed".

In a situation in which there are no gradients in the sediment transport rate per size fraction (and as such the mean bed elevation is constant in time), the only process that can lead to a change in surface composition is a change in elevation of the interface between the active layer and the substrate due to, for instance, an increase in the active-layer thickness. This is a limitation of the Hirano model, as several processes are inadequately described in this manner. For instance, lee-face sorting causes the deposition of coarse sediment at the dune troughs (Blom et al., 2003). As it often happens, the coarse sediment is immobile and dunes become composed of the fine sediment only. The coarse layer inhibits the entrainment of fine sediment and limits the sediment transport rate.

Although the formation of such a coarse layer is not modelled by the Hirano model, the Hirano model does account for the transport of some of the sediment fractions while some other sediment fractions remain immobile. Whether a particular sediment fraction is mobile or not, depends on the closure relation for the sediment transport rate (considering hiding and exposure) and the amount of the particular sediment fraction relative to the total sediment at the bed surface (i.e., in the active layer). The reduction in sediment transport is intrinsic to immobility of part of the sediment in the active.

A second important limitation is that, as we will see in Section 4, the flux between the active layer and the substrate yields physically unrealistic results when there is immobile sediment in the active layer. This is because, although sediment is immobile (i.e., it is too coarse to be transported) it moves vertically if the bed level increases, as sediment within the active layer moves with the bed level.

3. Proposed mathematical models

We propose two solutions for overcoming part of the limitations of the existing models. The first solution (Section 3.1) consists of a simple modification of Hirano's model.

The second one (Section 3.2) consists of extending the Hirano model by including a mixing layer below the active layer. This solution is inspired by the model developed by Tuijnder and Ribberink (2010a); Tuijnder et al. (2011) and Tuijnder and Ribberink (2012) for the formation of coarse layers under supply-limited conditions. Tuijnder et al. (2009) conducted a set of experiments in which bedforms grew from an initially-flat bed. A varying thickness of fine mobile sediment was placed over a layer of coarse immobile material. The height of the dunes that developed depended on the availability of mobile sediment. The modelling effort by Tuijnder and coauthors was intended at modelling this set of experiments. A review of the model revealed limitations that originated from its derivation specifically for the conditions of those laboratory experiments (Chavarrías et al., 2020).

3.1. ILSE model

In the Hirano model, the active layer follows the bed elevation. Assuming a constant active-layer thickness, this means that if there is a bed level increase (decrease), the sediment within the active layer moves upwards (downwards). If the active-layer thickness varies with time, the vertical movement is dependent on the variation of both the bed surface and the interface between the active layer and the substrate but in all cases there is vertical movement. The vertical movement of sediment is inherent to the assumption that the sediment in the active

layer is perfectly mixed and it is all equally available for being transported. As sediment deposits, it mixes with the sediment already present in the active layer. Hence, part of the deposited sediment is automatically present at the bottom of the new active layer, and part of the sediment in the original active layer is present in the top part of the new active layer. Similarly, as sediment is eroded, all the sediment in the active layer is equally available for being eroded.

In general, this is a good approximation of the undergoing physical processes as the active-layer thickness represents the part of the bed that is reworked by bedforms (Section 2.2). However, for the case in which immobile sediment is present in the active layer, it yields unrealistic results under aggradational conditions. In this case, immobile sediment is predicted to move upwards, whereas in reality it does not move.

Under degradational conditions it does not yield unrealistic results. Immobile sediment is predicted to move downwards as mobile sediment in the substrate enters the active layer. This models the case in which fine sediment is winnowed through the immobile sediment at the bed surface. Immobile sediment in the substrate also enters the active layer as degradation proceeds. As immobile sediment does not exit the active layer because it is not transported, there is an increase in the proportion of immobile sediment in the active layer, which inhibits further degradation (i.e., the bed is armoured).

In overcoming the limitation under aggradational conditions, a modification of the aggradational flux (Eq. (10)) is proposed. This is named the ILSE (ImmobiLe Sediment Exchange) model. As aggradation occurs, if there is immobile sediment in the active layer this is first transferred to the substrate. Immobile sediment is transferred proportional to its presence in the active layer. Once all sediment in the active layer is mobile, sediment transferred to the substrate has the same composition as that in the active layer.

Parameter k_{imm} is an index denoting the smallest immobile size fraction. Hence, grain sizes d_k with index $1 \leq k < k_{\mathrm{imm}}$ are mobile and grain sizes with index $k_{\mathrm{imm}} \leq k \leq N$ are immobile. The flux to the substrate is written as:

$$\Phi_{sk} = \frac{\partial z_s}{\partial t} \begin{cases} f_{sk1} & \text{for} \quad \frac{\partial z_s}{\partial t} < 0 \\ 0 & \text{for} \quad \frac{\partial z_s}{\partial t} > 0 \wedge \sum_{k=k_{\mathrm{imm}}}^{N} F_{ak} \neq 0 \wedge k < k_{\mathrm{imm}} \\ \dfrac{F_{ak}}{\sum_{k=k_{\mathrm{imm}}}^{N} F_{ak}} & \text{for} \quad \frac{\partial z_s}{\partial t} > 0 \wedge \sum_{k=k_{\mathrm{imm}}}^{N} F_{ak} \neq 0 \wedge k \geq k_{\mathrm{imm}} \\ \alpha_s F_{ak} + (1-\alpha_s) F_{bk} & \text{for} \quad \frac{\partial z_s}{\partial t} \geq 0 \wedge \sum_{k=k_{\mathrm{imm}}}^{N} F_{ak} = 0 \end{cases} \tag{12}$$

The first case in Eq. (12) considers degradational conditions. This is the same as in the Hirano model: substrate sediment is transferred to the active layer. The rest of the cases consider aggradational conditions. The second and third case consider the situation in which there is immobile sediment in the active layer. Under these conditions, mobile sediment is not transferred to the substrate (Case 2) and immobile sediment is transferred proportional to its presence in the active layer relative to all immobile sediment (Case 3). The fourth case considers aggradation when all sediment in the active layer is mobile. This last case is the same as that by Hoey and Ferguson (1994), which is equal to the standard Hirano model for $\alpha_s = 1$.

In stating that sediment size fractions are ordered in increasing size and that a particular index discerns between mobile and immobile fractions, we are implicitly assuming that reverse mobility does not occur (Solari and Parker, 2000). Reverse mobility occurs when the hiding-and-exposure effect is so strong that coarse fractions in the mixture are more mobile than fine ones (Dhamotharan et al., 1980; Misri et al., 1984; Kuhnle, 1993). Relaxation of this assumption is done by substituting the $1 \leq k < k_{\mathrm{imm}}$ by the indexes of the mobile fractions and $k_{\mathrm{imm}} \leq k \leq N$ by the indexes of the immobile ones.

3.2. HANNEKE model

3.2.1. Model description

An additional layer (named "coarse layer") is considered between the active layer and the substrate (Fig. 6). Variable z_{cl} [m] indicates the elevation of the top of the layer, L_{cl} [m] its thickness, F_{clk} [−] the volume fraction content of size fraction k, and M_{clk} the volume of sediment of size fraction k.

Immobile sediment in the active layer is transferred to the coarse layer at a certain rate, which causes a decrease of the active-layer thickness. Only mobile sediment is transferred from the coarse layer to the active layer. This process increases the active-layer thickness.

If the active-layer thickness is below a certain threshold L_{a0} [m], which is the active-layer thickness under alluvial conditions, there is a flux of mobile sediment (if present) from the coarse layer to the active layer at a certain rate.

If the active-layer thickness is smaller than the alluvial active-layer thickness, the sediment transport rate is reduced according to the relation by Struiksma (1999) (Eq. (3)). This models the fact that not all sediment at the bed surface can be transported. A fraction of the bed surface is covered by immobile sediment which means that the sediment transport rate as computed by the sediment transport closure relation applied to the mobile sediment needs to be reduced.

If the active-layer thickness has reached its alluvial value (hence there is no immobile sediment in it) and aggradation conditions are present, there is a transfer of mobile sediment from the active layer to the coarse layer such that the thickness of the active layer remains equal to its alluvial value.

If the active-layer thickness has reached its alluvial value (hence there is no immobile sediment in it) and degradation conditions are present and mobile sediment is available in the coarse layer, there is a flux of mobile sediment from the coarse layer to the active layer such that the thickness of the active layer remains equal to its alluvial value. In the case there is only immobile sediment available in the coarse layer, the active-layer thickness reduces.

The coarse layer has constant thickness, which simplifies the system of equations at the expenses of not capturing the complexity of the armouring process in detail. Further extension of the model should consider linking the coarse-layer thickness to, for instance, the thickness

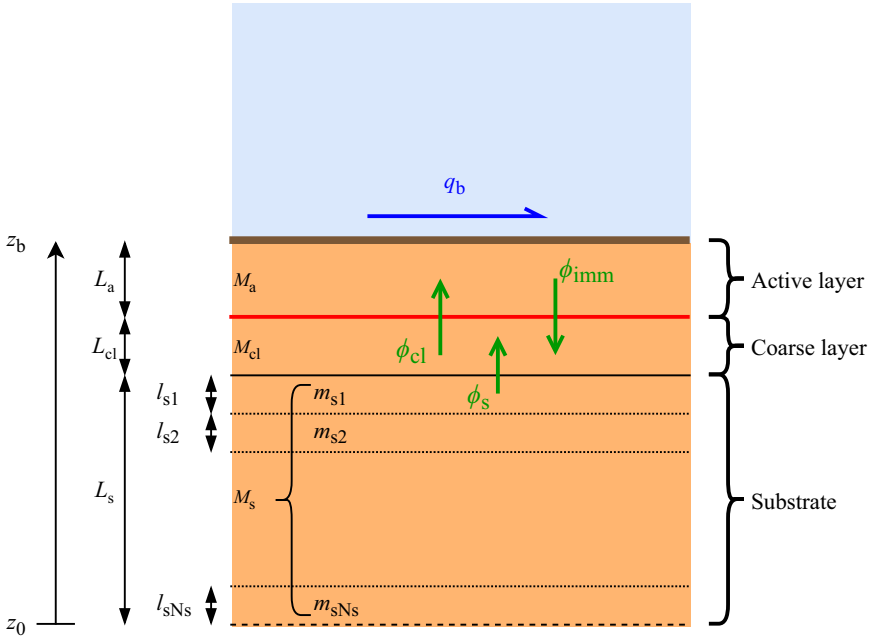

Fig. 6. Sketch of variables of HANNEKE model.

of the active layer or the properties of the sediment within it.

The flux of sediment between the coarse layer and the substrate is such that the thickness of the coarse layer is preserved.

We name this model HANNEKE (HirANo does Not havE the Key Exchange).

3.2.2. Conservation of mass

As with the previous models, the one-dimensional form is presented for simplicity, and the two-dimensional equations are obtained by considering the divergence of the sediment transport rate. Constant porosity is also assumed.

Mass conservation of the entire sediment mixture along the whole bed thickness is described by equation:

$$\frac{\partial z_b}{\partial t} + \frac{\partial \Psi_a q_b}{\partial x} = 0 \tag{13}$$

where $\Psi_a = L_a/L_{a0}$ [−] is the sediment transport reduction function by Struiksma (1999) applied to the active layer.

Mass conservation of the entire sediment mixture in the active layer is described by equation:

$$\frac{\partial L_a}{\partial t} + \frac{\partial \Psi_a q_b}{\partial x} + \Phi_{cl} - \Phi_{imm} = 0 \tag{14}$$

where Φ_{cl} [m/s] is the flux of sediment from the coarse layer to the active layer and Φ_{imm} [m/s] is the flux of immobile sediment from the active layer to the coarse layer (including pores).

As in the Hirano model, the divergence of the sediment transport rate is included in this control volume. This means that it includes the bed-load layer as defined by, for instance, Armanini and Di Silvio (1988). This also means that the fluxes related to entrainment of sediment into transport and deposition on the bed surface are not modelled and assumed instantaneous.

Mass conservation of the entire sediment mixture in the coarse layer is described by equation:

$$\frac{\partial L_{cl}}{\partial t} - \Phi_{cl} + \Phi_s + \Phi_{imm} = 0 \tag{15}$$

where Φ_s [m/s] is the flux of sediment from the substrate to the coarse layer.

Mass conservation of the entire sediment mixture in the substrate is described by equation:

$$\frac{\partial L_s}{\partial t} + \Phi_s = 0 \tag{16}$$

3.2.3. Conservation of mass per size fraction

Mass conservation per size fraction in the active layer is described by equation:

$$\frac{\partial M_{ak}}{\partial t} + \frac{\partial \Psi_a q_{bk}}{\partial x} + \Phi_{clk} - \Phi_{immk} = 0 \tag{17}$$

where Φ_{clk} [m/s] is the flux of size fraction k from the coarse layer to the active layer and Φ_{immk} [m/s] is the flux of immobile sediment of size fraction k from the active layer to the coarse layer. The grain-size-dependent fluxes are constrained by equations:

$$\Phi_{cl} = \sum_{k=1}^{N} \Phi_{clk} \tag{18}$$

$$\Phi_{imm} = \sum_{k=1}^{N} \Phi_{immk} \tag{19}$$

Mass conservation per size fraction in the coarse layer is described by equation:

$$\frac{\partial M_{clk}}{\partial t} - \Phi_{clk} + \Phi_{immk} + \Phi_{sk} = 0 \tag{20}$$

where Φ_{sk} [m/s] is the flux of size fraction k from the substrate to the coarse layer which is constrained by equation:

$$\Phi_s = \sum_{k=1}^{N} \Phi_{sk} \tag{21}$$

Mass conservation per size fraction in the substrate is described by equation:

$$\frac{\partial M_{sk}}{\partial t} - \Phi_{sk} = 0 \tag{22}$$

3.2.4. Sediment flux from the active layer to the coarse layer

The flux of immobile sediment from the active layer to the coarse layer depends on the amount such sediment in the active layer and the timescale at which it is transferred:

$$\Phi_{\mathrm{imm}} = \frac{L_{\mathrm{a}} \sum_{k=k_{\mathrm{imm}}}^{N} F_{ak}}{T_{\mathrm{imm}}} \tag{23}$$

where T_{imm} [s] is the timescale at which immobile sediment is transferred. Following Tuijnder and Ribberink (2010a), the transferring mechanism is deep dune troughs. Hence the timescale is associated to dune celerity and dune length, which are related to the sediment transport rate:

$$T_{\mathrm{imm}} = \frac{L_{\mathrm{a}} \Lambda}{q_{\mathrm{b}}} \tag{24}$$

where Λ [m] is the average dune length.

The average dune length Λ can be computed using one of the several empirical closure relations available to such an end. In the modelling software Delft3D (Walstra and Van Rijn, 2003; Lesser et al., 2004; Roelvink, 2006), two options are available. Van Rijn (1984b) proposes:

$$\Lambda = 7.3h \tag{25}$$

and a general power relation is implemented:

$$\Lambda = a_{\Lambda} h^{b_{\Lambda}} \tag{26}$$

where a_{Λ} [m] and b_{Λ} [1/m] are parameters and h [m] is the flow depth.

The flux per size fraction is:

$$\Phi_{\mathrm{imm}k} = \begin{cases} 0 & \text{for} \quad k < k_{imm} \\ \Phi_{imm} F_{ak} & \text{for} \quad k \geq k_{imm} \end{cases} \tag{27}$$

3.2.5. Sediment flux from the coarse layer to the active layer

Under the conditions in which the active-layer thickness is below the maximum alluvial value, the flux of mobile sediment from the coarse layer to the active layer depends on the amount such sediment in the coarse layer and the timescale at which it is transferred T_{cl} [s]. Under the conditions in which the active-layer thickness has reached its alluvial value (i.e., there is no immobile sediment in it) and aggradation occurs, sediment is transferred from the active layer to the coarse layer such that the thickness of the active layer remains constant. This implies that the mass flux is equal to the aggradational rate. Under the conditions in which the active-layer thickness has reached its alluvial value (i.e., there is no immobile sediment in it) and degradation occurs, mobile sediment is transferred from the coarse layer to the active layer such that the thickness of the active layer is constant:

$$\Phi_{\mathrm{cl}} = \begin{cases} \dfrac{L_{\mathrm{cl}} \sum_{k=1}^{k_{\mathrm{imm}}-1} F_{\mathrm{cl}k}}{T_{\mathrm{cl}}} & \text{for} \quad L_{\mathrm{a}} < L_{\mathrm{a},0} \\ -\dfrac{\partial q_{\mathrm{b}}}{\partial x} & \text{for} \quad L_{\mathrm{a}} = L_{\mathrm{a},0} \wedge \dfrac{\partial z_{\mathrm{b}}}{\partial t} \geq 0 \\ -\dfrac{\partial q_{\mathrm{b}}}{\partial x} & \text{for} \quad L_{\mathrm{a}} = L_{\mathrm{a},0} \wedge \dfrac{\partial z_{\mathrm{b}}}{\partial t} < 0 \wedge \sum_{k=1}^{k_{\mathrm{imm}-1}} F_{\mathrm{cl}k} > 0 \\ 0 & \text{for} \quad L_{\mathrm{a}} = L_{\mathrm{a},0} \wedge \dfrac{\partial z_{\mathrm{b}}}{\partial t} < 0 \wedge \sum_{k=1}^{k_{\mathrm{imm}-1}} F_{\mathrm{cl}k} = 0 \end{cases} \tag{28}$$

The flux per size fraction depends on the volume fraction content at the interface between the coarse layer and the active layer $f_k^{\mathrm{I,cl}}$ [−]:

$$\Phi_{\mathrm{cl}k} = \Phi_{\mathrm{cl}} f_k^{\mathrm{I,cl}} \tag{29}$$

where:

$$f_k^{\mathrm{I,cl}} = \begin{cases} F_{\mathrm{cl}k} & \text{for} \quad \left(L_{\mathrm{a}} < L_{\mathrm{a},0} \vee \dfrac{\partial z_{\mathrm{b}}}{\partial t} < 0 \right) \wedge k < k_{\mathrm{imm}} \\ F_{ak} & \text{for} \quad L_{\mathrm{a}} = L_{\mathrm{a},0} \wedge \dfrac{\partial z_{\mathrm{b}}}{\partial t} > 0 \end{cases} \tag{30}$$

Note that in the cases not specified, the flux is already zero so the volume fraction content is irrelevant.

In the current set-up, the timescale T_{cl} is assumed to be infinitely small, such that if the active-layer thickness is below the maximum alluvial value and there is mobile sediment in the coarse layer, this mobile sediment will be instantly mobilized and hence transferred to the active layer. From a numerical point of view, the timescale is equal to the time step and in one time step all mobile sediment is transferred to the active layer.

It is reasonable to think that the adaptation occurs at a certain timescale. This would model the fact that, under constant flow conditions, time is needed for the dune height (for which the active-layer thickness is proxy) to achieve the maximum value. This maximum value may be the alluvial value if enough sediment in the coarse layer is available or a lower value otherwise. This timescale of dune height adaptation can be modelled in several ways within Delft3D. Here a constant alluvial dune height has been employed for simplicity.

3.2.6. Sediment flux from the substrate to the coarse layer

The sediment flux from the substrate to the coarse layer guarantees that the thickness of the coarse layer remains constant:

$$\Phi_{\mathrm{s}} = \Phi_{\mathrm{cl}} - \Phi_{\mathrm{imm}} \tag{31}$$

The flux per size fraction depends on the sediment at the interface between the substrate and the coarse layer $f_k^{\mathrm{I,s}}$ [−]:

$$\Phi_{sk} = \Phi_{\mathrm{s}} f_k^{\mathrm{I,s}} \tag{32}$$

where:

$$f_k^{\mathrm{I,s}} = \begin{cases} f_{sk1} & \text{for} \quad \dfrac{\partial z_{\mathrm{s}}}{\partial t} < 0 \\ F_{\mathrm{cl}k} & \text{for} \quad \dfrac{\partial z_{\mathrm{s}}}{\partial t} \geq 0 \end{cases} \tag{33}$$

4. Application

4.1. Experimental set-up

The experiments by Struiksma (1999) are used for testing the different model concepts. The objective of these experiments was to measure the effect of a non-erodible layer in the propagation of a trench excavated in the bed. The data of two of his experiments are used here. The conditions were the same except for the fact that one was used as a reference and did not have a non-erodible layer installed.

Struiksma (1999) conducted his experiments in a 0.2 m wide, 0.5 m height flume with effective length equal to 11.5 m. Two sediment sizes were used; one mobile and one immobile. Mobile sediment was a uniform sand with characteristic grain size equal to 0.45 mm. Immobile sediment was a medium gravel in the range 8–16 mm. For modelling the coarse sediment the geometric mean grain size (11.3 mm) is used as characteristic grain size. Bed elevation profiles were measured manually using a rod. The discharge was measured using a sharp-crested weir and the water level downstream was controlled using a tailgate. The sediment transport rate was measured by collecting it at the downstream end of the flume. Both water and sediment were recirculated.

In each experiment, the flume was filled with approximately 0.15 m of sediment and it was run under constant a discharge and downstream water level until equilibrium conditions were obtained. Subsequently, a 2 m long 0.04 m deep trench was excavated and the experiment continued. In one of the experiments, a 3 m long fixed layer 0.016 m

Table 1
Modelled cases.

Case	Fine sediment	Coarse sediment	Initial composition of the bed surface
Low flow (Struiksma, 1999)	Mobile	Immobile	Fine sediment only
High flow (thought exp.)	Mobile	Mobile	Fine sediment only
Coarse layer formation (thought exp.)	Mobile	Immobile	Fine and coarse sediment

below the bed surface was present 1 m downstream from the trench, such that it became exposed as the trench propagated.

The discharge was equal to 9.2 l/s and the downstream water level was equal to 0.338 m above the flume bottom. This lead to a flow depth under normal flow conditions equal to 0.1 m, a water surface slope equal to 2.05×10^{-4}, and a sediment transport rate (without pores) equal to 5.83×10^{-6} m^2/s. The Chézy friction coefficient was 32.1 m$^{1/2}$/s.

This experiment, in which coarse sediment was immobile, is modelled in Section 4.3. A thought experiment equal except for the fact that the flow discharge (and, accordingly, the downstream water level for obtaining normal flow conditions) is higher is modelled in Section 4.4. In this latter case, coarse sediment is mobile. Finally, in Section 4.5 a second thought experiment is modelled resembling the situation after a flood wave passes. In this thought experiment the initial composition of the bed surface has both mobile and immobile sediment and considers a situation in which a coarse layer would form. The cases are summarized in Table 1.

4.2. Numerical modelling

Two different software have been used in modelling the experiments. The HANNEKE model has been implemented in a research branch of Delft3D. The ILSE model has been implemented in the research numerical model Elv (Chavarrías et al., 2019b). Both software have the Hirano and Struiksma models implemented.

Delft3D solves the unsteady shallow-water equations in 2D and 3D on curvilinear grids using an ADI (Alternate Direction Implicit) scheme. For this project a grid with only one cell in the transverse direction has been used essentially solving a 1D problem. Elv solves the Barré de Saint-Venant (1871) equations (i.e., unsteady 1D) using a Preissmann scheme with implicit parameter $\theta = 0.55$ (e.g. Lyn and Goodwin, 1987).

A 12 m long domain has been discretized with uniform space step equal to 0.05 m. 8 h are simulated. The time step is set to 0.1 s. Sediment and water density are equal to $\rho_s = 2650\,\mathrm{kg/m^3}$ and $\rho_w = 1000\,\mathrm{kg/m^3}$, respectively. Porosity is assumed to be $p = 0.4$. A Chézy friction type is used without flume-wall correction with the same value as described in the experiments. The sediment transport rate is modelled using the generalized relation by Meyer-Peter and Müller (1948):

$$Q_{bk} = \begin{cases} \dfrac{\sqrt{g\Delta d_k^3}}{1-p} A(\theta_k - \xi_k\theta_c)^B & \text{for } \theta_k - \xi_k\theta_c > 0 \\ 0 & \text{for } \theta_k - \xi_k\theta_c \le 0 \end{cases} \tag{34}$$

where Q_{bk} is the sediment transport capacity including pores (Eq. (6)), $g = 9.81\,\mathrm{m/s^2}$ is the acceleration due to gravity, $\Delta = (\rho_s - \rho_w)/\rho_w = 1.65$ is the relative sediment density, $\theta_k = u^2/(C^2\Delta d_k)$ [−] is the non-dimensional bed shear stress of size fraction k, $\theta_c = 0.047$ [−] is the critical non-dimensional bed shear stress, u [m/s] is the mean flow velocity, ξ_k [−] is the hiding-and-exposure coefficient, A [−] is the prefactor of the sediment transport relation, and $B = 1.5$ [−] is the power of the excess bed shear stress.

The prefactor A (which is equal to 8 in the original relation) has been calibrated for matching the measured transport under normal flow conditions leading to a value of 1.380835. The measured sediment transport does not allow for calibration of a hiding-and-exposure function. The function by Parker and Klingeman (1982):

$$\xi_k = \left(\frac{D_m}{d_k}\right)^b \tag{35}$$

where D_m [m] is the mean grain size and b [−] is a parameter has been used. The geometric mean grain size may better represent the mean properties of the mixture but as this is not implemented in Delft3D, the arithmetic mean grain size is used. A value $b = 0.2$ has been arbitrarily set such that the coarse sediment becomes mobile under the conditions of the thought experiment modelled in Section 4.4. Sediment mobility is computed based on the excess bed shear stress. A value $\theta_k - \xi_k\theta_c > 0$ indicates that size fraction k is mobile and vice versa.

Periodic boundary conditions for modelling sediment recirculation are not implemented in Delft3D. However, given the simulated time, the domain is long enough such that the effect of passing of the trench does not affect the downstream end of the domain. Hence, the load at the downstream end remains constant with time and as such a constant load at the upstream end equal to the load under normal flow conditions (i.e., 5.83×10^{-6} m^2/s without pores) has been imposed.

Struiksma (1999) considered the alluvial thickness to be 10% of the local flow depth. Here the alluvial thickness is set to a constant parameter equal to 0.01 m, which is the same as the value used by

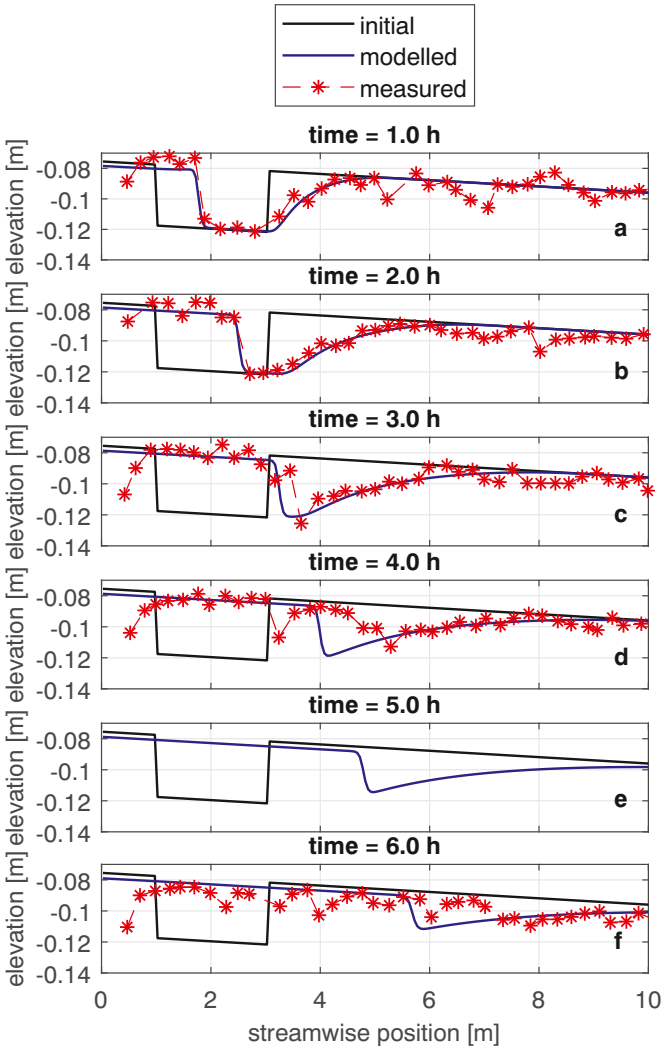

Fig. 7. Measured data and modelled results of the reference experiment (i.e., without a fixed layer) by Struiksma (1999). No measurements where available at 5 h.

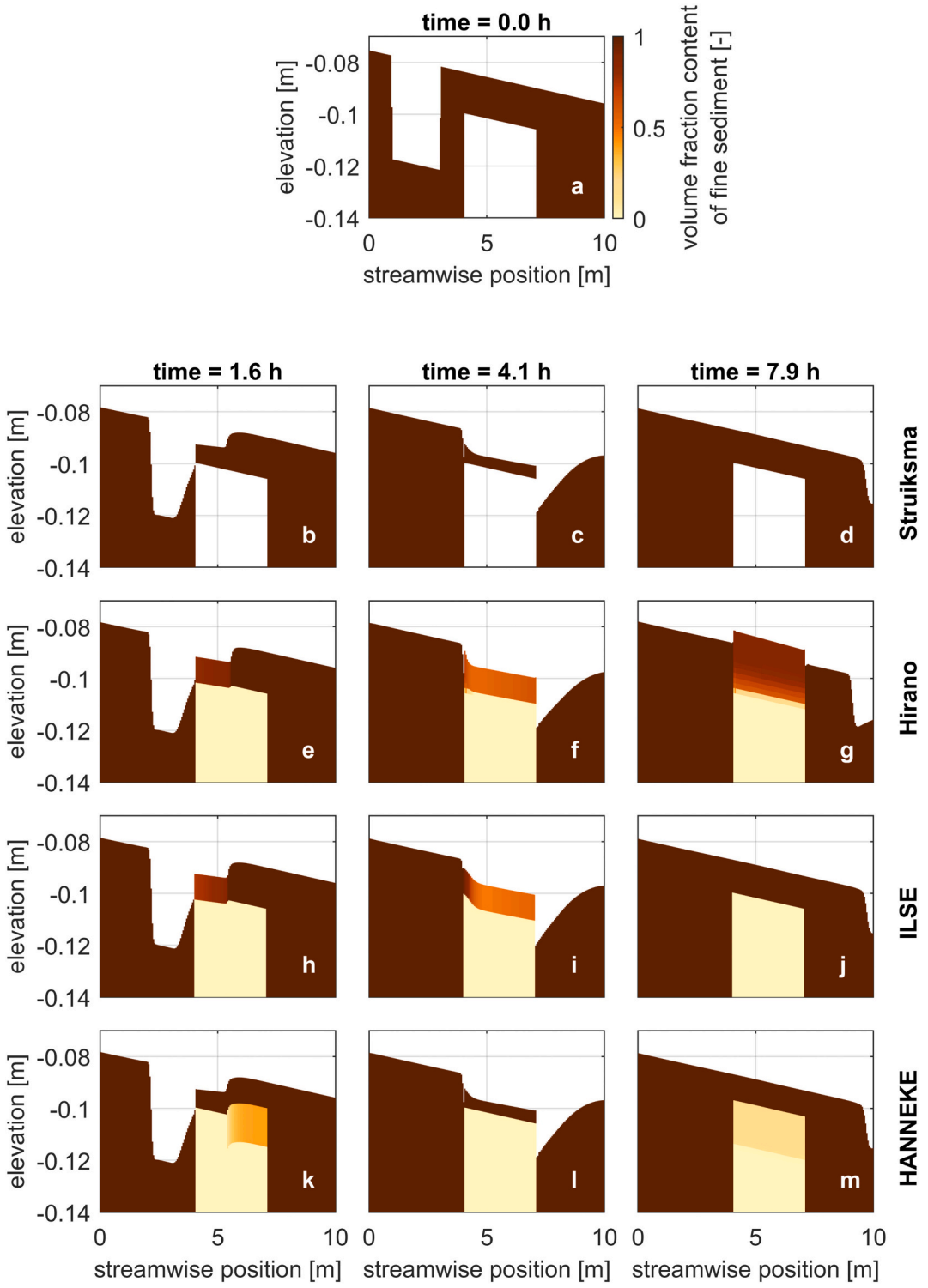

Fig. 8. Initial condition (**a**) and model results at different times (in columns) applying the model by Struiksma (top row), the model by Hirano (second row from above), the ILSE flux (third row from above) and the HANNEKE model (fourth row from above) to a case in which coarse sediment is immobile.

Struiksma (1999) for normal flow conditions. The active-layer thickness in the Hirano, ILSE, and HANNEKE models is also set to 0.01 m. This is reasonable considering the active-layer thickness to be $2D_{90}$ (Section 2.2). The substrate is discretized using 50 layers of 0.002 m in thickness.

In the HANNEKE model, the coarse-layer thickness is set to 0.015 m which is approximately 1.5 times the coarse-sediment characteristic grain size. The power relation for dune length (Eq. 26) is used with parameters $a_\Lambda = 0.5$ and $b_\Lambda = 0$ such that the dune length is set to a constant equal to 0.5 m.

Fig. 7 shows the measured data and the modelled results using Delft3D (the results using Elv are the same) of the reference experiment. As this is a uni-size simulation without a fixed layer, none of the model concepts presented are applied and it is only useful to show that the calibrated sediment transport relation (as well as all other numerical parameters) properly capture the dynamics of the experiment.

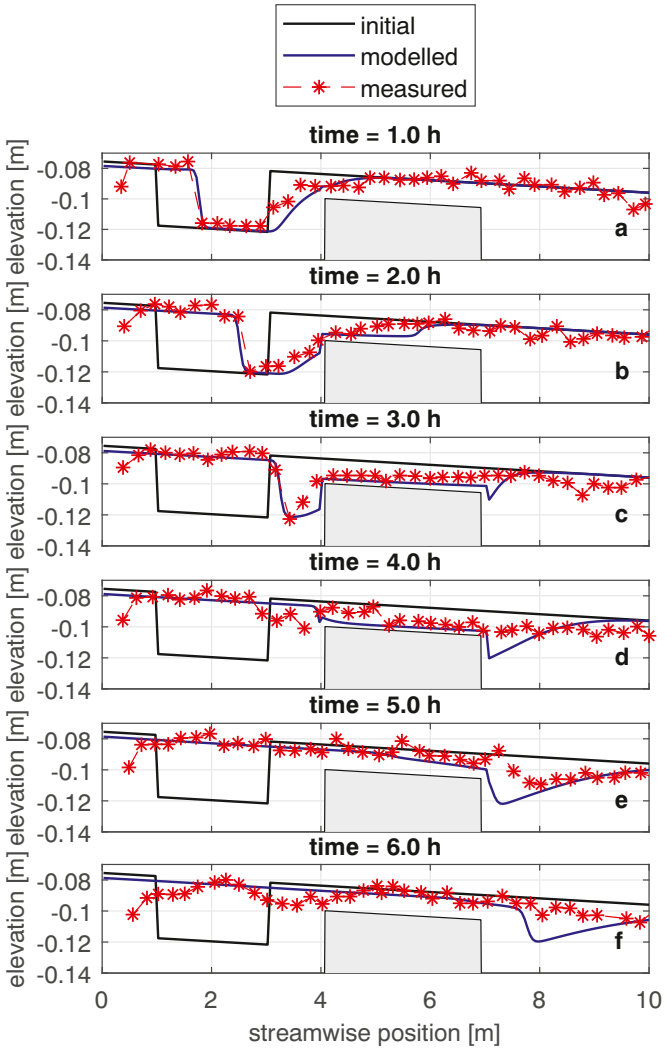

Fig. 9. Measured data of the experiment by Struiksma (1999) with a fixed layer and model results using the Struiksma model.

4.3. Low flow

In this section we show the results of applying the: (1) Struiksma, (2) Hirano, (3) ILSE, and (4) HANNEKE models to the experiment by Struiksma with a fixed layer (Fig. 8). The results of the model by Struiksma and Hirano are shown as computed with Delft3D and they are virtually identical when using Elv, as the only source of differences is due to numerical discretization details.

The model by Struiksma correctly represents the behaviour. Fig. 9 shows the results of this model together with measured data. The trench propagates downstream and disappears on top of the fixed layer for layer reappearing downstream. A key point is that after the trench has passed, the bed level is the same as initially. This is due to the fact that, both at the beginning and at the end of the run, the fixed layer is excessively deep to interact with the flow and the initial condition (without the trench) was at equilibrium.

Contrary to the model by Struiksma, the model by Hirano yields unrealistic results. The final bed elevation on the fixed layer is higher than initially (Fig. 8g). As the bed degrades, immobile sediment enters the active layer (Fig. 8e, f). This is to be interpreted as immobile sediment being exposed to the flow and it is realistic. The sediment transport rate of fine sediment on the fixed layer is reduced as the volume fraction content of fine sediment reduces due to an increase in the presence of coarse sediment (see Eq. (6)). As the bed level increases, sediment in the active layer moves upwards following the bed level. Hence, immobile sediment in the active layer moves upwards too. This causes that, after the trench has passed, immobile sediment is found at a higher elevation that it was initially. A part of the coarse sediment that entered the active layer has been re-deposited in the substrate in the aggradation process. However, as the depositional flux is proportional to the presence in the active layer (Eq. (10)), part of that flux is fine sediment, while in reality it should only be formed out of coarse sediment.

By using the aggradational flux by Hoey and Ferguson (1994) (Eq. (11)) the problem would only be increased, as a larger fraction of fine sediment would be transferred to the substrate considering that the load is formed out of fine sediment only.

The final configuration depends on the hiding-and-exposure parameters. A larger hiding-and-exposure effect implies that the presence of coarse sediment further limits the transport of fine sediment, which causes a larger unrealistic final aggradation. Nevertheless, even without considering the role of hiding and exposure, the final bed level is unrealistic, as the mere presence of coarse sediment in the active layer causes a reduction of the transport of fine sediment.

The ILSE model overcomes the problem of the model by Hirano and yields realistic results. Coarse sediment enters the active layer as degradation occurs (Fig. 8h, i). However, contrary to the Hirano model, in the final state the bed surface is formed out of fine sediment only (Fig. 8j). This is because, as aggradation proceeds, immobile sediment deposits first, as if assuming that it is in the lowest part of the active layer. The final result when using the ILSE model is identical to that obtained when using Struiksma's model. However, while in Struiksma's case the fixed layer is modelled as a non-erodible layer, when using the ILSE model the fixed layer is composed of coarse immobile sediment.

The HANNEKE model also yields realistic results. No step in bed level is found and the final bed slope is the equilibrium slope. As the trench propagates on the fixed layer, immobile sediment does not enter the active layer, hence mimicking the behaviour of the model by Struiksma (compare Fig. 8l to Fig. 8c). The active layer is always formed out of fine sediment. Hence, in the final state coarse sediment is not found at the bed surface which yields a realistic bed elevation profile.

Fig. 10 shows the geometric mean grain size of the sediment in the active layer and in the coarse layer at the middle of the layer of coarse sediment ($x = 5.525$ m) with time. The grain size of the sediment in the active layer does not change with time as coarse sediment does not enter it. Sediment in the coarse layer is initially coarser than the sediment in the active layer as part of the coarse layer includes immobile sediment from the start. The coarse layer gradually coarsens during the first approximately 1.5 h as the bed level lowers and there is sufficient fine sediment in the coarse layer. In this case, the active-layer thickness remains constant which implies that the coarse layer lowers while entraining coarse sediment from the substrate. The proportion of coarse sediment (and the mean grain size) increases. Once no more fine sediment is available in the coarse layer, further degradation occurs at the expenses of the active-layer thickness. In this case the coarse layer does not change elevation and no fluxes of sediment occur. As a consequence, the mean grain size remains constant. After approximately 4.5 h of experiment, aggradation occurs. Fine sediment enters the coarse layer as this moves upwards, which causes a fining of the coarse layer.

In the final state when using the ILSE model, the substrate has the exact same composition as initially. On the contrary, the substrate shows a gradient in fraction of immobile sediment when using the HANNEKE model. This is because immobile sediment has entered the coarse layer and has been transported upwards during the aggradation phase. This is unrealistic, although it does not affect the final state as sediment in the coarse layer does not interact with the flow. Fig. 10 shows this entrance of immobile sediment as the coarse layer is initially finer than at the end.

4.4. High flow

In this section the results of applying the four presented models to a

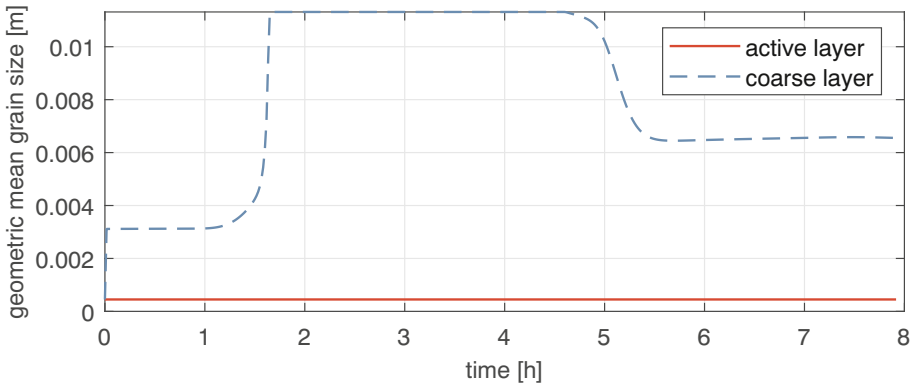

Fig. 10. Geometric mean grain size of the sediment in the active layer (red continuous line) and in the coarse layer (blue dashed line) at $x = 5.525$ m with time in a case in which coarse sediment is immobile.

thought experiment in which all sediment is mobile are presented. The conditions are the same as the ones explained in Section 4.1 except for the fact that the discharge is 10 times larger (i.e., 92 l/s). The initial bed elevation has been adjusted such that initially the normal flow depth (equal to 0.465 m) prevails (except for the trench). The sediment load under normal flow conditions (i.e., without the trench) is equal to 7.36×10^{-5} m^2/s.

Fig. 11 shows the results. The Struiksma model does not predict entrainment of the coarse sediment, as this is modelled as a non-erodible layer. The results of the Hirano model are identical to those of the ILSE model. This is not surprising as the flux to and from the substrate is identical in both cases when all sediment is mobile.

Finally the HANNEKE model predicts very similar results to those of the Hirano model. Nevertheless, while in the Hirano model, the substrate lays directly below the active layer, in the HANNEKE model there is an extra layer moving with the bed level (i.e., the coarse layer). The coarse layer is in this case 7.5 times thicker than the substrate layers, which causes the observed discretization differences.

Fig. 12 shows the change in time of the mean grain size in the coarse layer. There is an initial (first 1 h) coarsening phase of the coarse layer. Similarly to the previous case (Section 4.3) degradation occurs and coarse sediment from the substrate enters the coarse layer. Contrary to the previous case, the active layer also coarsens as all sediment (i.e., including the coarse fraction) from the coarse layer is transferred to the active layer. Subsequently, the active layer becomes finer as it aggrades and only fine sediment arrives from upstream. The coarse layer also becomes finer as it moves upwards and fine sediment is transferred from the active to the coarse layer.

4.5. Coarse layer formation

This application consist of modelling of a second thought experiment in which a coarse layer is formed under constant discharge and normal flow conditions. A situation after a flood wave is considered. Sediment that is immobile prior to a flood wave is mobilized during the flood wave and is found at the bed surface (i.e., interacting with the flow) when the flood wave recedes and becomes immobile again.

The modelled conditions are identical to those in the experiment by Struiksma (Section 4.1) except for the fact that no fixed layer nor trench are installed. Moreover, the bed surface is initially composed of 50% of fine sediment and 50% of coarse sediment. For simulating periodic boundary conditions (relevant for the HANNEKE model in which the composition changes), a first preparatory simulation is run with a constant load and a second simulation is run imposing the load at the downstream end from the first simulation.

Fig. 13 shows the results of applying the different modelling concepts. The Hirano model does not predict any changes in bed elevation or composition (Fig. 13e, f, g). The sediment transport rate is the same everywhere since the start of the simulation (i.e., uniform). Hence, there are no changes in bed elevation. Moreover, as the only source of vertical sediment fluxes is a change in bed elevation (considering that the active-layer thickness is constant), the composition also remains constant.

Note that a decrease in the active-layer thickness would never lead to a change in composition. Moreover, in the case we model, an increase in the active-layer thickness would also not lead to a change in composition as the substrate sediment has the same composition as the active layer.

We conclude that the Hirano model does not explicitly predict the formation of a coarse layer. Nevertheless, it is relevant to note that only fine sediment is transported while the bed surface is composed of 50% of coarse sediment. The partial mobility indicates that the bed is probably armoured.

Struiksma's model cannot be applied in this context, as there is no layer composed of only immobile sediment. Worded differently, there is no non-erodible layer. Immobile sediment is since the beginning at the bed surface and the model does not predict the formation of a non-erodible layer.

The ILSE model only causes a different result than the Hirano model under aggradational conditions. As no changes in bed elevation occur, the ILSE model predicts the same results than the Hirano model. In essence, there is no explicit modelling of the formation of a coarse layer.

The HANNEKE model does predict changes in composition (Fig. 13k, l,m). The situation is initially uniform and changes are also uniform (i.e., the same changes occur at every position in the streamwise direction). Hence, while the sediment transport rate changes with time, the gradient in sediment transport rate is always equal to 0 along the entire domain and there are no changes in bed elevation.

Immobile coarse sediment initially present in the active layer sinks to the coarse layer and mobile sediment in the coarse layer is transferred to the active layer. With time, the active layer becomes finer and the coarse layer becomes coarser (Fig. 14). Because the coarse layer is 1.5 times as thick as the active layer and initially all layers are composed of 50% of each type of sediment, all coarse sediment initially in the active layer can be transferred to the coarse layer without reducing the active-layer thickness.

If the coarse layer would have been finer than the active layer, immobile sediment in the active layer would have been transferred to the coarse layer but the coarse layer would not supply mobile sediment to the active layer. Hence, the thickness of the active layer would have reduced. In this case, the coarse layer moves upwards and immobile sediment is transferred to the substrate. Eventually, the active layer would be formed out of mobile sediment only; the coarse layer would be formed out of immobile sediment only; and the situation would also reach equilibrium.

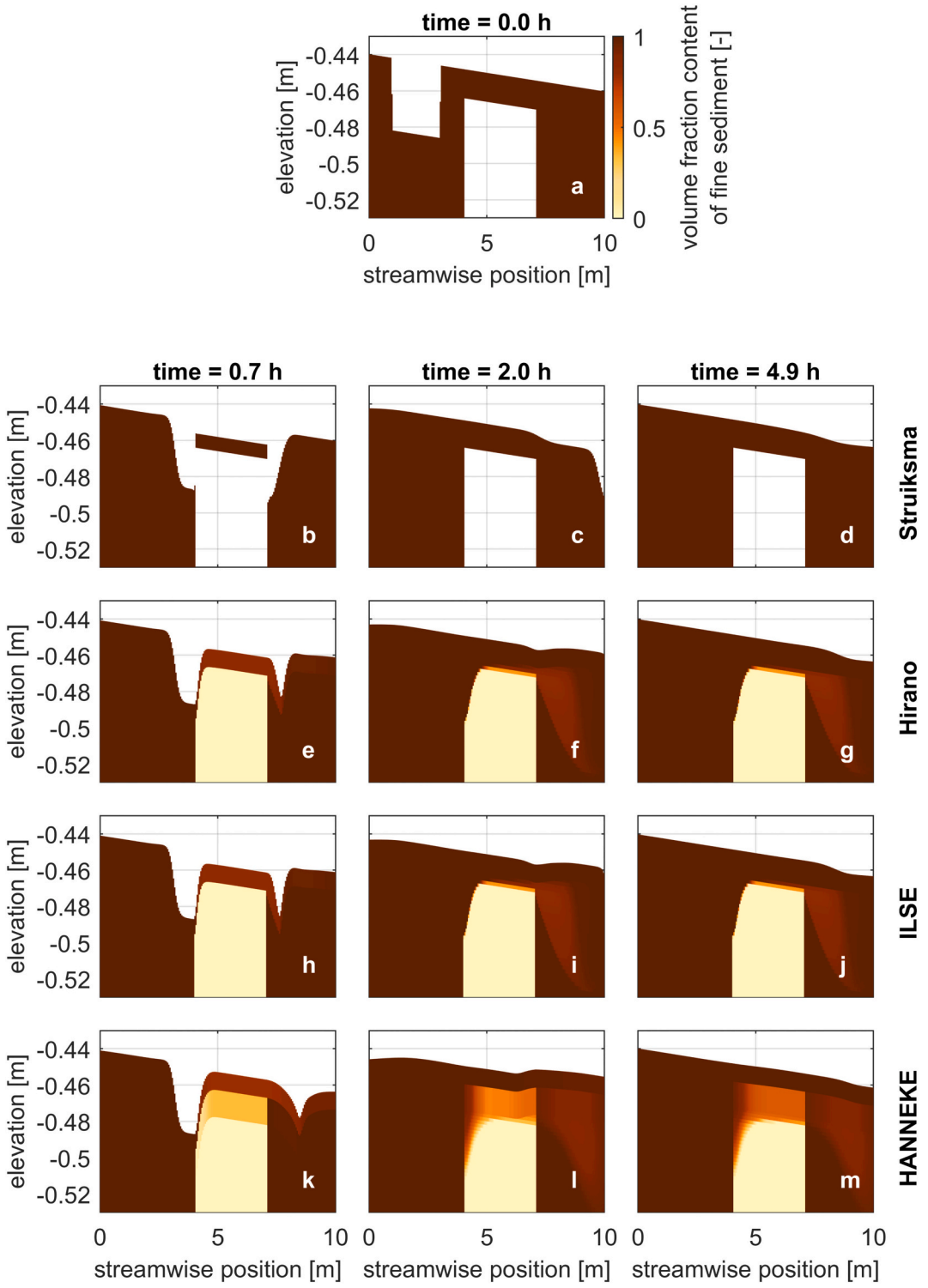

Fig. 11. Initial condition (**a**) and model results at different times (in columns) applying the model by Struiksma (top row), the model by Hirano (second row from above), the ILSE model (third row from above) and the HANNEKE model (fourth row from above) to a case in which all sediment is mobile.

5. Discussion

5.1. Model capabilities

The Struiksma model can reproduce morphodynamic development in the presence of a non-erodible layer (i.e., formed by immobile sediment). However, it fails to model break-up of a coarse layer. On the contrary, the Hirano model yields physically unrealistic results in the presence of an immobile sediment layer, but it captures break-up of such a layer. The results are summarized in Table 2.

Both the ILSE and HANNEKE models correctly predict morphodynamic development in the presence of an immobile sediment layer. However, they achieve this in fundamentally different manners. While in the ILSE model immobile sediment in the substrate enters the active layer, in the HANNEKE model immobile sediment does not enter the active layer. In the HANNEKE model the thickness of the active layer

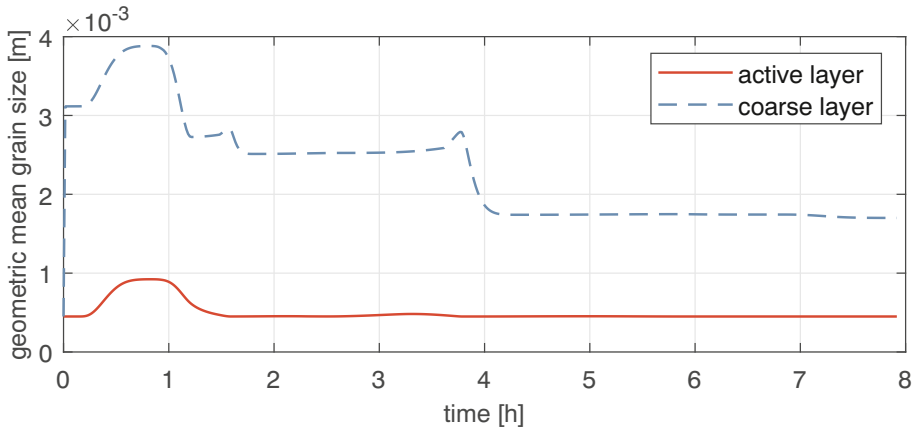

Fig. 12. Geometric mean grain size of the sediment in the active layer (red continuous line) and in the coarse layer (blue dashed line) at $x = 5.525$ m with time in a case in which all sediment is mobile.

reduces as there is a lack of mobile sediment, while when using the ILSE model the active-layer thickness remains constant.

The different model behaviour highlights the crucial point that the active layer represents different properties in each model. In the ILSE model (as in the Hirano model), the active layer represents the part of the bed that interacts with the flow, better described in a probabilistic manner (Section 2.2). Immobile sediment exposed to the flow is then part of the active layer.

In the HANNEKE model, sediment in the active layer not only interacts with the flow but is also regularly mobilized. Sediment in the active layer may not be in transport but is mobilized periodically by passing bedforms.

This is similar to the case of the Struiksma model in which the thickness of sediment above a non-erodible layer plays the role of the active layer in the HANNEKE model. The alluvial thickness in Struiksma's model is equivalent to the alluvial active-layer thickness in the HANNEKE model. Moreover, it is the alluvial active-layer thickness and not the active-layer thickness in the HANNEKE model that has a closest correspondence with the active-layer thickness in the Hirano and ILSE models.

Regarding modelling of the formation of a coarse layer, only the HANNEKE model explicitly reproduces this process. Nevertheless, the Hirano and ILSE models implicitly describe the formation of a coarse layer. A coarse layer is present if the active layer contains immobile sediment. Worded differently, the bed is armoured if there is a sediment size fraction which is in the active layer but not transported. Although a decrease in flow velocity suddenly causing coarse sediment to stop being transported does not cause a change in bed surface composition (Section 4.5), the change in sediment transport rate implicitly models the formation of the coarse layer.

5.2. Presence of immobile sediment in the active layer

Immobile sediment enters the active layer in the Hirano and ILSE models but not in the HANNEKE model and both approaches correctly reproduce the physical processes. Both manners of modelling the same process are valid and it is a matter of how to interpret the results (Section 5.1). Nevertheless, the fact that in the HANNEKE model immobile sediment does not enter the active layer and is transferred out of it if present, causes the model to have certain limitations.

First is that at least some sediment must be mobile. Otherwise, the active-layer thickness would tend to be 0, which would imply infinitely fast changes in bed surface composition, as the celerity of changes inversely depends on the active-layer thickness (Ribberink, 1987; Stecca et al., 2014; Chavarrías et al., 2019b). This is not only physically unrealistic but also numerically challenging.

Second is that it is necessary to discern between mobile and immobile sediment. This model necessity prevents using sediment transport relations which do not include a threshold for motion such as Engelund and Hansen (1967) and Wilcock and Crowe (2003). One could use such a load relation and independently discern between mobile and immobile sediment using a criterion such as Shields (1936). This is not recommended as it yields physically unrealistic results. Sediment in the active layer which is transported would sink to the coarse layer and stop being transported if labelled as immobile by the mobility criterion.

The third limitation is also related to sediment mobility. In the HANNEKE model, the properties of the coarse layer are not considered in computing the sediment transport rate although sediment in the coarse layer is exposed to the flow and interacts with it. As a corollary, although one may consider the hiding-and-exposure effect in the sediment transport relation, this does not consider the grain size of the immobile sediment in the coarse layer, although it certainly affects the mobility of the fine sediment. The effect of hiding and exposure is implicitly considered in the sediment transport reduction function (i.e., Ψ_a in Eqs. (13) and (14)). It could be possible to improve the model by, for instance, computing hiding and exposure using a mean grain size based on the sediment in both the active layer and the coarse layer. Furthermore, the whole sediment transport rate could be computed as a weighted average of the sediment in the active layer and coarse layer. This would yield similar results to the Hirano model, in which the sediment in the coarse layer falls inside the active layer. This would make the sediment transport reduction function redundant and unnecessary. Still, an important limitation remains that applies to the four models: the usual sediment transport relations (e.g. Engelund and Hansen, 1967; Meyer-Peter and Müller, 1948; Ashida and Michiue, 1971; Wilcock and Crowe, 2003) and hiding-and-exposure functions (e.g. Egiazaroff, 1965; Ashida and Michiue, 1971; Parker et al., 1982; Wilcock and Crowe, 2003) have not been derived for conditions of high bi-modality and large differences in grain size such as the ones we have modelled here. Research is needed that focuses on estimating the sediment transport rate under these conditions.

5.3. Ill-posedness

A last point regarding model capabilities is about ill-posedness of the system of equations. The Hirano model is ill-posed under certain circumstances, particularly when degrading into a substrate finer than the active layer (Ribberink, 1987; Stecca et al., 2014; Chavarrías et al., 2018, 2019c). When the model is ill-posed, spurious oscillations scaling with the grid size develop which artificially mix sediment and can even cause failure of the numerical solver. Ill-posedness arises from the simplifications inherent to the model conceptualization and is not a

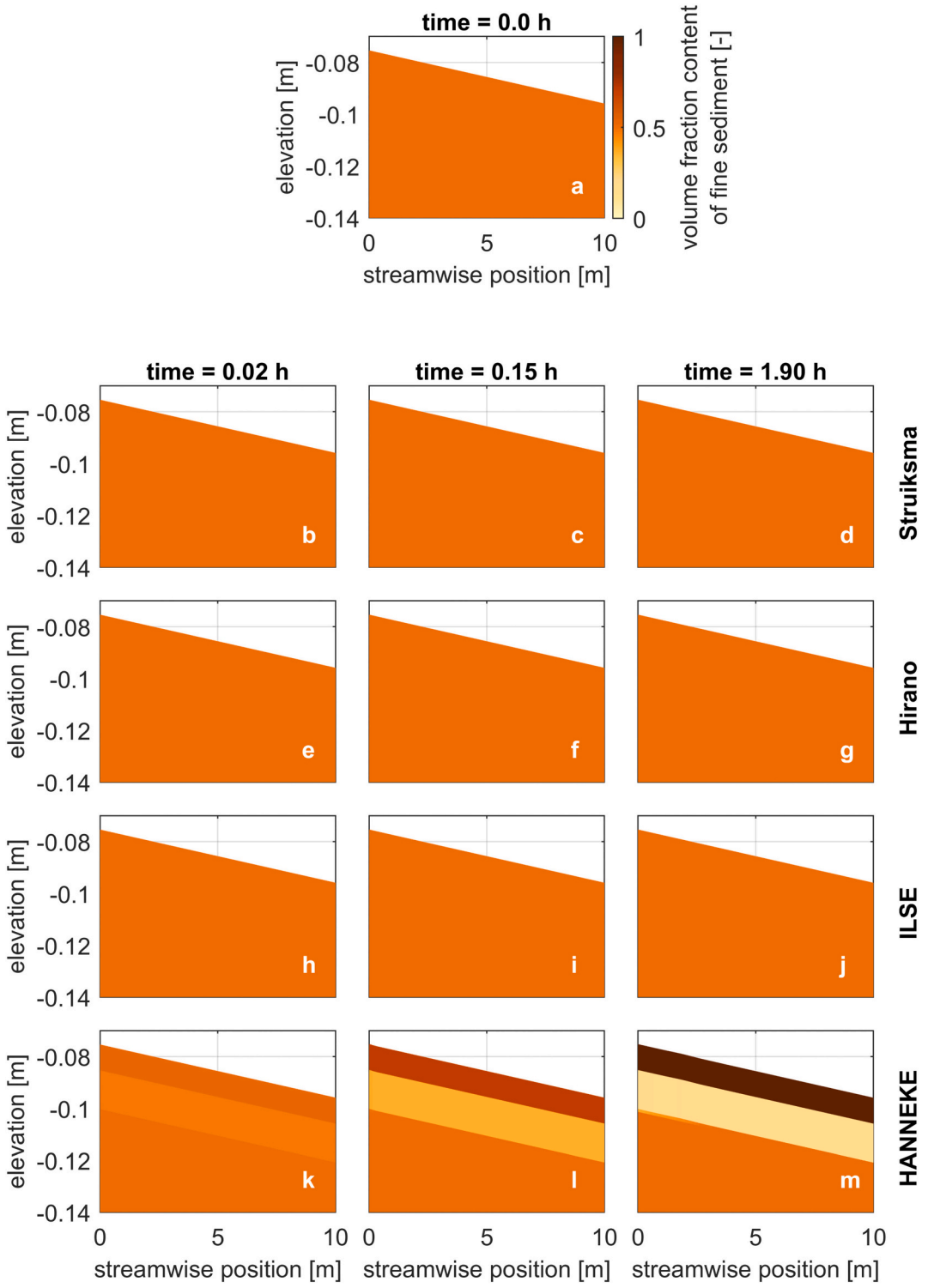

Fig. 13. Initial condition (**a**) and model results at different times (in columns) applying the model by Struiksma (top row), the model by Hirano (second row from above), the ILSE model (third row from above) and the HANNEKE model (fourth row from above) to a case in which coarse sediment initially in the active layer is immobile.

numerical artefact.

The ILSE model is equivalent to the Hirano model under degradational conditions. Hence, under the degradational conditions in which the Hirano model is ill-posed, the ILSE model will also be ill-posed. Under aggradational conditions, the interface between the active layer and the substrate in the ILSE model is equal or coarser than the interface in the Hirano model. This reduces the likelihood that the ILSE model becomes ill-posed. Still, the most relevant case is the degradational one so we conclude that the ILSE model does not in general pose a solution to the problem of ill-posedness.

In the HANNEKE model the coarse layer acts as a buffer between the active layer and the substrate. If the coarse layer is fully formed and degradation occurs by a decrease in the active-layer thickness, there is no flux of sediment between the coarse layer and the active layer and the

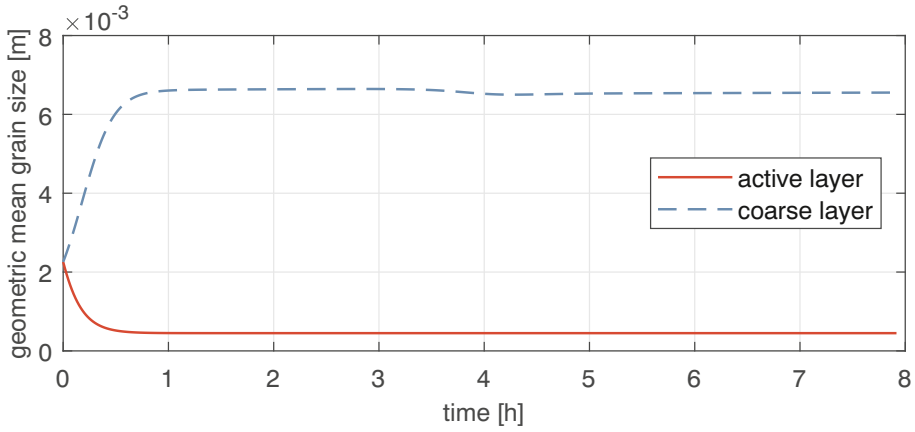

Fig. 14. Geometric mean grain size of the sediment in the active layer (red continuous line) and in the coarse layer (blue dashed line) at $x = 5.525$ m with time in a case in which coarse sediment initially in the active layer is immobile.

Table 2
Model capabilities.

Model	Transport over a coarse layer	Coarse-layer break-up	Explicit coarse-layer formation
Struiksma	yes	no	no
Hirano	no	yes	no
ILSE	yes	yes	no
HANNEKE	yes	yes	yes

model is well-posed. A case in which all sediment is mobile and degradation occurs into a fine substrate will not differ from the Hirano model and will equally be ill-posed (if the Hirano model is ill-posed). However, if there is immobile sediment in the coarse layer while degrading, the proportion of fine sediment entering the active layer will be smaller and it is less likely that the HANNEKE model will become ill-posed.

In conclusion, although we provide no formal proof, we expect that the HANNEKE model has a smaller domain of ill-posedness than the Hirano model. Still, we are certain that it is not unconditionally well-posed. The SILKE model (Chavarrías et al., 2019a) provides an alternative unconditionally well-posed model. However, the SILKE model is computationally more expensive as it requires solving an additional advection-diffusion equation for each grain size and the time step must be smaller in order to capture a faster timescale. Moreover, it suffers from the problems of immobile sediment modelling solved using the ILSE and HANNEKE models.

Another alternative is the regularized Hirano model (Chavarrías et al., 2019b). The regularization can be seen as a modification of the timescale of the mixing processes that guarantees well-posedness while preserving the framework of the Hirano model not adding additional conservation equations. While being more expensive than the standard Hirano model, it is less expensive than the SILKE model.

It would be possible to extend the SILKE and regularized Hirano models with the concepts of the ILSE or HANNEKE models for better modelling immobile sediment.

5.4. Model choice

Several modelling options have been presented for considering mixed-size sediment processes. While one single option clearly better than the rest would facilitate modelling, we find that each model has its own domain of application and it depends on the case which model is better. Here we provide guidelines for selecting the appropriate model.

We do not recommend using the Hirano model, as the ILSE model represents a small modification of it which only improves it without drawbacks.

If modelling the effect of an engineered fixed layer made with sediment much coarser than the alluvial sediment or, for instance, concrete, we would recommend using the Struiksma model. This is better than the ILSE model because in the latter the coarse sediment enters the active layer and affects the sediment transport of the alluvial sediment while the current sediment-transport and hiding-and-exposure relations are not fit for these cases. It would also be possible to use the HANNEKE model but it would increase the complexity without additional benefits.

In a case in which all sediment can be immobile or the preferred sediment transport relation does not include a mobility threshold, the HANNEKE model is not recommended, as in the former the model yields unrealistic results and in the latter adds complexity without additional benefits. The ILSE model is the preferred option.

If the interest lays on modelling the dynamics of sediment as this becomes mobile and immobile, the key point is whether the explicit coarse-layer formation is a process of interest. If indeed the timescale of formation of a coarse layer is of interest, the only choice is the HANNEKE model. If one is not interested in this process, the ILSE model provides a simpler alternative.

Finally, if the situation can be ill-posed and the dynamics of immobile sediment are relevant, one either has to use an extended SILKE model or a regularized ILSE or HANNEKE model. The choice would depend on whether one is interested in the short-timescale mixing waves occurring under these circumstances. Only the SILKE model resolves such waves. If only the overall behaviour is of interest, the regularized ILSE and HANNEKE models are better options due to their reduced computational time.

6. Conclusion

Accurate modelling of morphodynamic development under conditions in which part of the sediment is immobile is crucial for river management. By modelling a laboratory experiment and two thought experiments, we have shown that the two existing models of Struiksma and Hirano present severe limitations. The Struiksma model is incapable of modelling formation and break-up of an armour layer and the Hirano model yields physically unrealistic results when part of the sediment is immobile. We have proposed the ILSE and HANNEKE models for overcoming these limitations. The two models differ in the interpretation of the active layer in which sediment interacts with the flow. The ILSE model is a simple modification of the Hirano model in which the flux of sediment between the active layer and the substrate is improved for correctly capturing the dynamics under aggradational conditions. We have found that this improved flux is sufficient for modelling a case in which part of the sediment is immobile. The HANNEKE model includes a layer below the active layer where immobile sediment is deposited. This

additional layer allows for explicit modelling of the formation of an armoured layer. This is a unique feature of the HANNEKE model, as the alternatives model the formation in an implicit manner.

Declaration of competing interest

The authors declare that they have no known competing financial interests or personal relationships that could have appeared to influence the work reported in this paper.

Acknowledgements

This project is part of the KPP Rivierkunde programme at Deltares, funded by Rijkswaterstaat. We thank Arjan Sieben and Rien van Zetten for their valuable feedback on the model improvements. We thank two anonymous reviewers for their critical comments that substantially improved the manuscript.

References

Armanini, A., 1995. Non-uniform sediment transport: dynamics of the active layer. J. Hydraul. Res. 33 (5), 611–622. https://doi.org/10.1080/00221689509498560.
Armanini, A., di Silvio, G., 1988. A one-dimensional model for the transport of a sediment mixture in non-equilibrium conditions. J. Hydraul. Res. 26 (3), 275–292. https://doi.org/10.1080/00221688809499212.
Arnaud, F., Piégay, H., Schmitt, L., Rollet, A.J., Ferrier, V., Béal, D., 2015. Historical geomorphic analysis (1932–2011) of a by-passed river reach in process-based restoration perspectives: the Old Rhine downstream of the Kembs diversion dam (France, Germany). Geomorphology 236, 163–177. https://doi.org/10.1016/j.geomorph.2015.02.009.
Arnaud, F., Piégay, H., Béal, D., Collery, P., Vaudor, L., Rollet, A.-J., 2017. Monitoring gravel augmentation in a large regulated river and implications for process-based restoration. Earth Surf. Process. Landf. 42 (13), 2147–2166. https://doi.org/10.1002/esp.4161.
Ashida, K., Michiue, M., 1971. An investigation of river bed degradation downstream of a dam. In: Proc. of the 14th IAHR World Congress, 29 August–3 September, Paris, France, vol. 3, pp. 247–255.
Barré de Saint-Venant, A.J.C., 1871. Théorie du mouvement non permanent des eaux, avec application aux crues des rivières et a l'introduction des marées dans leur lit. C. R. Seances Acad. Sci. 73, 237–240 (in French).
Becker, A., 2017. Advies uitvoering en monitoring 2e suppletie Bovenrijn, Tech. Rep. 11200877-000-ZWS-0003. Deltares, Delft, the Netherlands, 100 pp.
Bell, R.G., Sutherland, A.J., 1983. Nonequilibrium bedload transport by steady flows. J. Hydraul. Eng. 109 (3), 351–367. https://doi.org/10.1061/(ASCE)0733-9429(1983)109:3(351).
Bennett, J.P., Nordin, C.F., 1977. Simulation of sediment transport and armouring. Hydrol. Sci. Bull. 22 (4), 555–569. https://doi.org/10.1080/02626667709491760.
Blom, A., Ribberink, J.S., de Vriend, H.J., 2003. Vertical sorting in bed forms: flume experiments with a natural and a trimodal sediment mixture. Water Resour. Res. 39 (2), 1025. https://doi.org/10.1029/2001WR001088.
Bravard, J.-P., Kondolf, G.M., Piégay, H., 1999. Environmental and societal effects of river incision and remedial strategies. In: Simon, A., Darby, S.E. (Eds.), Incised River Channels. Wiley, Chichester, pp. 303–341.
Carling, Gölz, Orr, Radecki-Pawlik, 2000. The morphodynamics of fluvial sand dunes in the River Rhine, near Mainz, Germany. I. Sedimentology and morphology. Sedimentology 47 (1), 227–252. https://doi.org/10.1046/j.1365-3091.2000.00290.x.
Carling, Williams, Göz, Kelsey, 2000. The morphodynamics of fluvial sand dunes in the River Rhine, near Mainz, Germany. II. Hydrodynamics and sediment transport. Sedimentology 47 (1), 253–278. https://doi.org/10.1046/j.1365-3091.2000.00291.x.
Chavarrías, V., Stecca, G., Blom, A., 2018. Ill-posedness in modelling mixed-sediment river morphodynamics. Adv. Water Resour. 114, 219–235. https://doi.org/10.1016/j.advwatres.2018.02.011.
Chavarrías, V., Arkesteijn, L., Blom, A., 2019a. A well-posed alternative to the Hirano active layer model for rivers with mixed-size sediment. J. Geophys. Res. Earth Surf. 124 (11), 2491–2520. https://doi.org/10.1029/2019JF005081.
Chavarrías, V., Stecca, G., Siviglia, A., Blom, A., 2019b. A regularization strategy for modeling mixed-sediment river morphodynamics. Adv. Water Resour. 127, 291–309. https://doi.org/10.1016/j.advwatres.2019.04.001.
Chavarrías, V., Schielen, R., Ottevanger, W., Blom, A., 2019c. Ill posedness in modelling two-dimensional morphodynamic problems: effects of bed slope and secondary flow. J. Fluid Mech. 868, 461–500. https://doi.org/10.1017/jfm.2019.166.
Chavarrías, V., Ottevanger, W., Mosselman, E., 2020. Morphodynamic Modelling Over Alluvial and Non-alluvial Layers. Literature Review, Update to Tuijnder Concept, Tech. Rep. 11205235-016-ZWS-0006_v0.1. Deltares, Delft, the Netherlands, 73 pp.
Colombini, M., 2004. Revisiting the linear theory of sand dune formation. J. Fluid Mech. 502, 1–16. https://doi.org/10.1017/S0022112003007201.
Colombini, M., Stocchino, A., 2005. Coupling or decoupling bed and flow dynamics: fast and slow sediment waves at high Froude numbers. Phys. Fluids 17 (3). https://doi.org/10.1063/1.1848731, 036,602.
Cui, Y., 2007. The unified gravel-sand (TUGS) model: simulating sediment transport and gravel/sand grain size distributions in gravel-bedded rivers. Water Resour. Res. 43 (10) https://doi.org/10.1029/2006WR005330. W10,436.
de Jong, J., Ottevanger, W., 2020. Analyse van de bodemhoogte Rijntakken van 1999 tot 2018, Tech. Rep. 11202744-003-ZWS-0001. Deltares, Delft, the Netherlands, 5 pp.
Deigaard, R., Fredsøe, J., 1978. Longitudinal grain sorting by current in alluvial streams. Nord. Hydrol. 9 (1), 7–16. https://doi.org/10.2166/nh.1978.002.
Dhamotharan, S., Wood, A., Parker, G., Stefan, H., 1980. Bedload Transport in a Model Gravel Strem, Tech. Rep. 190. St. Anthony Falls Hydraulic Laboratory, University of Minnesota, Minneapolis, MN, United States, 71 pp.
Die Moran, A., El Kadi Abderrezzak, K., Mosselman, E., Habersack, H., Lebert, F., Aelbrecht, D., Laperrousaz, E., 2013. Physical model experiments for sediment supply to the Old Rhine through induced bank erosion. Int. J. Sediment Res. 28 (4), 431–447. https://doi.org/10.1016/S1001-6279(14)60003-2.
Egiazaroff, I.V., 1965. Calculation of nonuniform sediment concentrations. J. Hydraul. Div. 91 (4), 225–247.
Einstein, H.A., 1950. The Bed-load Function for Sediment Transportation in Open Channel Flows, Tech. Bull, 1026. US Department of Agriculture, Soil Conservation Service, Washington, DC, United States, 70 pp.
Engelund, F., Hansen, E., 1967. Monograph on Sediment Transport in Alluvial Streams, Tech. Rep. Hydraulics Laboratory, Technical University of Denmark, Copenhagen, Denmark, 63 pp.
Exner, F.M., 1920 (2a). In: Zur Physik der Dünen, Akad. Wiss. Wien Math. Naturwiss, 129, pp. 929–952 (in German).
Garegnani, G., Rosatti, G., Bonaventura, L., 2011. Free surface flows over mobile bed: mathematical analysis and numerical modeling of coupled and decoupled approaches. Commun. Appl. Ind. Math. 2 (1), e371 https://doi.org/10.1685/journal.caim.371.
Garegnani, G., Rosatti, G., Bonaventura, L., 2013. On the range of validity of the Exner-based models for mobile-bed river flow simulations. J. Hydraul. Res. 51 (4), 380–391. https://doi.org/10.1080/00221686.2013.791647.
Havinga, H., 2020. Towards sustainable river management of the Dutch Rhine River. Water 12 (1827). https://doi.org/10.3390/w12061827.
Hirano, M., 1971. River bed degradation with armoring. Proc. Jpn Soc. Civ. Eng. 195, 55–65. https://doi.org/10.2208/jscej1969.1971.195_55.
Hoey, T.B., Ferguson, R.I., 1994. Numerical simulation of downstream fining by selective transport in gravel bed rivers: model development and illustration. Water Resour. Res. 30 (7), 2251–2260. https://doi.org/10.1029/94WR00556.
Holly, F.M., Rahuel, J.L., 1990. New numerical/physical framework for mobile-bed modelling. J. Hydraul. Res. 28 (4), 401–416. https://doi.org/10.1080/00221689009499057.
Hu, P., Xian Cao, Z., Pender, G., Han Liu, H., 2014. Numerical modelling of riverbed grain size stratigraphic evolution. Int. J. Sediment Res. 29 (3), 329–343. https://doi.org/10.1016/S1001-6279(14) 60048-2.
Jain, S.C., 1992. Note on lag in bedload discharge. J. Hydraul. Eng. 118 (6), 904–917. https://doi.org/10.1061/(ASCE)0733-9429(1992)118:6(904).
Karim, M.F., Holly, F.M., 1986. Armoring and sorting simulation in alluvial rivers. J. Hydraul. Eng. 112 (8), 705–715. https://doi.org/10.1061/(ASCE)0733-9429(1986)112:8(705).
Klaassen, G.J., 1987. Armoured River Beds During Floods, Tech. Rep, 394. Delft Hydraulics Laboratory, Delft, the Netherlands.
Klaassen, G.J., Tukker, H., Driegen, J., van der Woude, G., 1986. Morfologie afgepleisterde beddingen: proeven met hoogwatergolven, Tech. Rep. M2061/Q212. Delft Hydraulics Laboratory, Delft, the Netherlands (in Dutch).
Kuhnle, R.A., 1993. Incipient motion of sand-gravel sediment mixtures. J. Hydraul. Eng. 119 (12), 1400–1415. https://doi.org/10.1061/(ASCE)0733-9429(1993)119:12(1400).
Lee, H.-Y., Odgaard, A.J., 1986. Simulation of bed armoring in alluvial channels. J. Hydraul. Eng. 112 (9), 794–801. https://doi.org/10.1061/(ASCE)0733-9429(1986)112:9(794).
Lesser, G.R., Roelvink, J.A., van Kester, J.A.T.M., Stelling, G.S., 2004. Development and validation of a three-dimensional morphological model. Coast. Eng. 51 (8–9), 883–915. https://doi.org/10.1016/j.coastaleng.2004.07.014.
Luu, X.L., Takebayashi, H., Egashira, S., 2004. Characteristics of sediment sorting predicted by two different exchange layer models. Jpn. Soc. Fluid Mech. A225, 248–249.
Lyn, D.A., Goodwin, P., 1987. Stability of a general Preissmann scheme. J. Hydraul. Eng. 113 (1), 16–28. https://doi.org/10.1061/(ASCE)0733-9429(1987)113:1(16).
Meyer-Peter, E., Müller, R., 1948. Formulas for bed-load transport. In: Proc. 2nd IAHR World Congress, 6–9 June, Stockholm, Sweden, pp. 39–64.
Misri, R.L., Garde, R.J., Raju, K.G.R., 1984. Bed load transport of coarse nonuniform sediment. J. Hydraul. Eng. 110 (3), 312–328. https://doi.org/10.1061/(ASCE)0733-9429(1984)110:3(312).
Mosselman, E., Kerssens, P., van der Knaap, F., Schwanenberg, D., Sloff, K., 2004. Sustainable River Fairway Maintenance and Improvement, Tech. Rep. Q3757.00. Delft Hydraulics Laboratory, Delft, the Netherlands. https://doi.org/10.13140/RG.2.1.3728.5606.
Paola, C., Voller, V.R., 2005. A generalized Exner equation for sediment mass balance. J. Geophys. Res. Earth Surf. 110 (F4) https://doi.org/10.1029/2004JF000274. F04,014.
Papanicolaou, A.N., Bdour, A., Wicklein, E., 2004. One-dimensional hydrodynamic/sediment transport model applicable to steep mountain streams. J. Hydraul. Res. 42 (4), 357–375. https://doi.org/10.1080/00221686.2004.9728402.

Parker, G., 1991. Selective sorting and abrasion of river gravel. I: Theory. J. Hydraul. Eng. 117 (2), 131–147. https://doi.org/10.1061/(ASCE)0733-9429(1991)117:2(131).
Parker, G., Klingeman, P.C., 1982. On why gravel bed streams are paved. Water Resour. Res. 18 (5), 1409–1423. https://doi.org/10.1029/WR018i005p01409.
Parker, G., Sutherland, A.J., 1990. Fluvial armor. J. Hydraul. Res. 28 (5), 529–544. https://doi.org/10.1080/00221689009499044.
Parker, G., Klingeman, P.C., McLean, D.G., 1982. Bedload and size distribution in paved gravel-bed streams. J. Hydraul. Div. 108 (4), 544–571.
Peters, B., Dittrich, A., Stoesser, T., Smits, T., Geerling, G., 2001. The Restrhine: New Opportunities for Nature Rehabilitation and Flood Prevention, Tech. Rep. University of Nijmegen, the Netherlands and University of Karlsruhe, Germany.
Petts, G.E., Thoms, M.C., Brittan, K., Atkin, B., 1989. A freeze-coring technique applied to pollution by fine sediments in gravel-bed rivers. Sci. Total Environ. 84, 259–272. https://doi.org/10.1016/0048-9697(89)90388-4.
Rahuel, J., Holly, F., Chollet, J., Belleudy, P., Yang, G., 1989. Modeling of riverbed evolution for bedload sediment mixtures. J. Hydraul. Eng. 115 (11), 1521–1542. https://doi.org/10.1061/(ASCE)0733-9429(1989)115:11(1521).
Ribberink, J.S., 1987. Mathematical Modelling of One-dimensional Morphological Changes in Rivers With Non-uniform Sediment. Delft University of Technology, Delft, the Netherlands. Ph.D. thesis.
Roelvink, J.A., 2006. Coastal morphodynamic evolution techniques. Coast. Eng. 53 (2–3), 277–287. https://doi.org/10.1016/j.coastaleng.2005.10.015.
Shields, A., 1936. Anwendung der Ähnlichkeitsmechanik und Turbulenzforschung auf die Geschiebebewegung. Ph.D. thesis, 26. Versuchsanstalt für Wasserbau und Schiffbau, Berlin, Germany (in German).
Siele, M., Blom, A., Viparelli, E., 2019. Two counterintuitive findings on channel bed incision in engineered alluvial rivers. In: Friedrich, H., Bryan, K. (Eds.), 11th Symposium on River, Coastal and Estuarine Morphodynamics, Auckland, New Zealand 16–21 November, p. 143.
Sloff, K., Mosselman, E., 2012. Bifurcation modelling in a meandering gravel-sand bed river. Earth Surf. Process. Landf. 37 (14), 1556–1566. https://doi.org/10.1002/esp.3305.
Sloff, C.J., Mosselman, E., Sieben, J., 2006. Effective use of non-erodible layers for improving navigability. In: Ferreira, R.M.L., Alves, E.C.T.L., Leal, J.G.A.B., Cardoso, A.H. (Eds.), Proceedings of the 3rd International Conference on Fluvial Hydraulics (River Flow), Lisbon, Portugal, 6-8 September. Taylor and Francis, London, United Kingdom, pp. 1211–1220.
Solari, L., Parker, G., 2000. The curious case of mobility reversal in sediment mixtures. J. Hydraul. Eng. 126 (3), 185–197. https://doi.org/10.1061/(ASCE)0733-9429(2000)126:3(185).
Staentzel, C., Arnaud, F., Combroux, I., Schmitt, L., Trémolières, M., Grac, C., Piégay, H., Barillier, A., Chardon, V., Beisel, J.-N., 2018. How do instream flow increase and gravel augmentation impact biological communities in large rivers: a case study on the Upper Rhine River. River Res. Appl. 34 (2), 153–164. https://doi.org/10.1002/rra.3237.
Stecca, G., Siviglia, A., Blom, A., 2014. Mathematical analysis of the Saint-Venant-Hirano model for mixed-sediment morphodynamics. Water Resour. Res. 50 (10), 7563–7589. https://doi.org/10.1002/2014WR015251.
Struiksma, N., 1999. Mathematical modelling of bedload transport over non-erodible layers. In: Proceedings of the 1st IAHR Symposium on River, Coastal, and Estuarine Morphoynamics, Genova, Italy, pp. 89–98.
Tuijnder, A., Ribberink, J., 2010. A Morphological Concept for Semi-fixed Layers, Tech. Rep. 2011R-003/WEM-003. Twente University, Enschede, the Netherlands, 31 pp.
Tuijnder, A., Ribberink, J.S., 2010. Development of supply-limited transport due to vertical sorting of a sand-gravel mixture. In: Muñoz, R. Murillo (Ed.), Proceedings of the 5th International Conference on Fluvial Hydraulics (River Flow), Braunschweig, Germany, 8-10 September. CRC press, Taylor and Francis Group, pp. 487–492.
Tuijnder, A., Ribberink, J.S., 2012. Immobile layer formation due to vertical sorting of immobile grain size fractions. In: Koll, K., Dittrich, A., Aberle, J., Geisenhainer, P. (Eds.), Proceedings of the 6th International Conference on Fluvial Hydraulics (River Flow), San José, Costa Rica, 5-7 September. Bundesanstalt für Wasserbau, Karlsruhe, Germany, pp. 847–854.
Tuijnder, A.P., Ribberink, J.S., Hulscher, S.J.M.H., 2009. An experimental study into the geometry of supply-limited dunes. Sedimentology 56 (6), 1713–1727. https://doi.org/10.1111/j.1365-3091.2009.01054.x.
Tuijnder, A., Ribberink, J., Spruyt, A., 2011. Modelling Semi-fixed Layers With Delft3D, Tech. Rep. 2011R-004/WEM-004. Twente University, Enschede, the Netherlands.
van Niekerk, A., Vogel, K.R., Slingerland, R.L., Bridge, J.S., 1992. Routing of heterogeneous sediments over movable bed: model development. J. Hydraul. Eng. 118 (2), 246–262. https://doi.org/10.1061/(ASCE)0733-9429(1992)118:2(246).
van Rijn, L.C., 1984a. Sediment transport, part I: bed load transport. J. Hydraul. Eng. 110 (10), 1431–1456. https://doi.org/10.1061/(ASCE)0733-9429(1984)110:10(1431).
van Rijn, L.C., 1984b. Sediment transport, part III: bed forms and alluvial roughness. J. Hydraul. Eng. 110 (12), 1733–1754. https://doi.org/10.1061/(ASCE)0733-9429(1984)110:12(1733).
Visser, P.J., 2000. Bodemontwikkeling Rijnsysteem: Een verkenning van omvang, oorzaken, toekomstige ontwikkelingen en mogelijke maatregelen (Bed Development of the Rhine System: An Exploration of Magnitude, Causes, Future Developments and Possible Measures), Report to Rijkswaterstaat Oost-Nederland. Delft University of Technology, Delft, the Netherlands (in Dutch).
Vreugdenhil, C.B., 1994. Numerical Methods for Shallow-Water Flow. Springer, Dordrecht, the Netherlands. https://doi.org/10.1007/978-94-015-8354-1, 262 pp.
Walstra, D.J., van Rijn, L.C., 2003. Modeling of Sand Transport in Delft3D, Tech. Rep. Z3624. Delft Hydraulics Laboratory, Delft, the Netherlands.
Wilcock, P.R., Crowe, J.C., 2003. Surface-based transport model for mixed-size sediment. J. Hydraul. Eng. 129 (2), 120–128. https://doi.org/10.1061/(ASCE)0733-9429(2003)129:2(120).
Wu, W., 2004. Depth-averaged two-dimensional numerical modeling of unsteady flow and nonuniform sediment transport in open channels. J. Hydraul. Eng. 130 (10), 1013–1024. https://doi.org/10.1061/(ASCE)0733-9429(2004)130:10(1013).
Wu, F., Yang, K., 2004. Entrainment probabilities of mixed-size sediment incorporating nearbed coherent flow structures. J. Hydraul. Eng. 130 (12), 1187–1197. https://doi.org/10.1061/(ASCE)0733-9429(2004)130:12(1187).